8-2011

Accurate circuit model for predicting the performance of lead-acid AGM batteries

Wenxin Peng
University of Nevada, Las Vegas

ACCURATE CIRCUIT MODEL FOR PREDICTING THE PERFORMANCE OF LEAD-ACID AGM BATTERIES

by

Wenxin Peng

Bachelor of Science
Tongji University, China
2009

A thesis submitted in partial fulfillment
of the requirements for the

Master of Science Degree in Electrical Engineering
Department of Electrical and Computer Engineering
Howard R. Hughes College of Engineering

Graduate College
University of Nevada, Las Vegas
August 2011

THE GRADUATE COLLEGE

We recommend the thesis prepared under our supervision by

Wenxin Peng

entitled

Accurate Circuit Model for Predicting the Performance of Lead-Acid AGM Batteries

be accepted in partial fulfillment of the requirements for the degree of

Master of Science in Electrical Engineering
Department of Electrical and Computer Engineering

Yahia Baghzouz, Committee Chair

Henry Selvaraj, Committee Member

Ramasubramanian Venkatasubramanian, Committee Member

Robert Boehm, Graduate College Representative

Ronald Smith, Ph. D., Vice President for Research and Graduate Studies
and Dean of the Graduate College

August 2011

ABSTRACT

Accurate Circuit Model for Predicting the Performance of Lead-Acid AGM Batteries

by

Wenxin Peng

Dr. Yahia Baghzouz, Examination Committee Chair
Professor of
Department of Electrical and Computer Engineering
University of Nevada, Las Vegas

Energy storage technologies are becoming of great importance in many modern electrical systems. In particular, electrochemical batteries are rapidly gaining wide-spread application in transportation systems as well as in the electric utility sector, where they provide a means to convert non-dispatchable renewable resources into dispatchable generation sources. Hence, accurate battery models are needed during the design stage of such systems to forecast future performance.

A variety of models with a varying degree of complexity and accuracy currently exist that predict battery behavior. In the proposed paper, an existing battery model is modified to account for some battery irregularities while maintaining simplicity is proposed to represent a sealed AGM battery. The model consists of controlled sources, resistors, and capacitors. The nonlinear relationship between the State of Charge (SOC) and the open circuit voltage (VOC) of the battery is accounted for. The values of the circuit parameters are derived using the curves provided in the manufacturer's data sheet as well as some simple laboratory tests on a 12 V, 89 Ah battery.

A comparison between the measured and simulated (using Matlab/Simulink) responses to various charge/discharge cycles shows a comfortable degree of accuracy of the proposed battery model.

ACKNOWLEDGMENTS

I would like to express my sincerely gratitude to Dr. Baghzouz for his encouragement, guidance, time and dedication to keep me on the right track throughout these two years. His excellence in both research and teaching will always be a great example to me.

Also, I would like to thank Dr. Venkat and Dr. Selvaraj for serving as committee members and Dr. Boehm for serving as graduate faculty representative.

Last but not least, I would like to thank my family and friends for their care and mental support that make me achieve my goal.

TABLE OF CONTENTS

LIST OF FIGURES

CHAPTER 1

INTRODUCTION

1.1 Thesis Objective

An absorbed glass mat (AGM) battery is a class of valve-regulated lead-acid (VRLA) battery, which is designed for low-maintenance rechargeable batteries. AGM batteries are almost the same as lead-acid battery except the electrolyte is held in glass mat separators, as opposed to freely flooding the plates. This design brings significant advantages to AGM batteries such as purer lead, water conservation, fluid retention, high power density, lower internal resistance that allow the batteries being charged or discharged more quickly, etc.

As a result, the voltage performance of AGM during charging and discharging is slightly different from conventional lead-acid batteries. From the manufacturer's datasheet it can be seen how the open circuit changes with the DOD (Depth of Discharge) increasing. The purpose of this thesis is to develop an accurate circuit model, with the internal resistance value carefully obtained by simple lab tests.

In the proposed paper the phenomenon is observed that as the discharging current rises, the resonation of the internal circuit becomes obvious. In Fig.1, the dip of the curves becomes more and more visible as the hour-rate changing from 120HR to 1HR. This is mainly caused by the polarization effect of the battery which can not be easily explained. Some of the research uses empirical function by adding an exponential expression to the model, but most of the research on battery modeling neglected this effect. Considering this effect has little influence to the modeling results, it will not be discussed in the following chapters.

The circuit model for lead-acid batteries has been widely developed in the past decades; most of them contain a controlled voltage source and a resistor with several RC circuits in series to predict the battery behavior in constant current conditions as well as transient reactions. A good review of this kind of model is presented by Ng in 2008. That paper showed a simplified equivalent circuit and derived some equations mainly for state of charge (SOC) and terminal voltage, which matches the experimental results in certain extent. Another good paper is presented by Chen in 2006, it showed an electric model for all kinds of batteries and gave out detailed simulation results and derivations for all the parameters during the test, and a pulse sequence of input current was applied. Medora developed two model using manufacturer's data. The purpose of most battery model research is for application to electric vehicle batteries.

This thesis will demonstrate a more accurate circuit model for lead-acid AGM batteries, based on one of the existing model mentioned above with extension and improvements. Temperature effects will be considered and a detailed defined battery function will be given.

A nice battery model will help improving the research of fast-charging scheme for car batteries, which is crucial for electric vehicles or solar electric refueling stations, and also the battery storage technology itself. The parameters of this proposed model are case-specific because the model is not developed under chemical level, the factor that affects SOC and open circuit voltage changes when applied to another type of battery like Li-ion or Ni-M, even to lead-acid but made up in different structure or different concentration of chemical components. A feasible way to extend it to a universal battery model is establishing a data base to restore every set of parameters which applies to this model.

1.2 Organization of the Thesis

This thesis is organized into seven chapters.

Chapter 2 is a brief introduction about lead acid battery by explaining its theory and technical definitions.

Chapter 3 explains the details for how to develop the circuit model for a battery.

Chapter 4 and 5 state the experiments and analyze the results. Tests and measurements are taken in the lab and simulations are carried out using Matlab and MS-OFFICE software.

Chapter 6 discusses the temperature effect on batteries as a supplement for the conclusions of previous chapters and shows the finalized circuit model. Analysis and applications of the model are also presented.

CHAPTER 2

LITERATURE REVIEW

2.1 The Theory of the Lead-acid Storage Battery

The lead storage battery is the most conventional and the most widely applied storage battery in the world today. Applications for these vary from small sealed batteries of a few Watt-hours capacity in consumer applications to large batteries of many megawatt-hours capacity in submarines, utilities, and other applications.

The reaction products at the electrodes on charge and discharge of a lead-acid storage battery are given in the "double sulfate theory":

$$PbO_2 + Pb + 2H_2SO_4 \overset{Charge/Discharge}{\longleftrightarrow} 2PbSO_4 + 2H_2O(l)$$

(Gladstone and Tribe, 1881-1883). The enthalpy, Gibbs free energy and its temperature coefficients for this chemical reaction have been the subject of many discussions. Because the concentration of sulfuric acid is appreciably changed by the conversion, numerous investigations of its thermodynamics have been carried out. Since 1954 these studies have been extended by two important findings:

1. The discovery of two forms of PbO_2, α- PbO_2, β- PbO_2, in the active materials leads to alterations in the value of the thermodynamic quantities. The free energies of the two modifications of PbO_2 differ slightly, whereas the entropies are quite different.
2. The electrochemistry of the materials existing between defined phase limits (e.g., lead dioxide) can be explained. The breadth of the phase influences the potential.

A lead acid battery uses a combination of lead plates or grids and an electrolyte consisting of a diluted sulfuric acid to convert electrical energy into potential chemical energy and back again. Each cell of a lead acid battery contains (in the charged state) electrodes of lead metal (Pb) and lead (IV) oxide (PbO_2) in an electrolyte of about 37% w/w (5.99 Molar) sulfuric acid (H_2SO_4). In the discharged state both electrodes turn into lead (II) sulfate ($PbSO_4$) and the electrolyte loses its dissolved sulfuric acid and becomes primarily water. Due to the freezing-point depression of water, as the battery discharges and the concentration of sulfuric acid decreases, the electrolyte is more likely to freeze. Because of the open cells with liquid electrolyte in most lead-acid batteries, overcharging with excessive charging voltages will generate oxygen and hydrogen gas by electrolysis of water, forming an explosive mix. This should be avoided. Caution must also be observed because of the extremely corrosive nature of sulfuric acid.

Lead acid batteries have lead plates for the two electrodes. Separators are used between the positive and negative plates of a lead acid battery to prevent short-circuit through physical contact, mostly through dendrites (‘treeing’), but also through shedding of the active material. Separators obstruct the flow of ions between the plates and increase the internal resistance of the cell.

2.2 Technical Definitions of Lead-acid Storage Battery

A galvanic cell is a combination of two electrodes and electrolyte that permits the production of useful electrical work by chemical reaction. Two types of cell (primary and secondary or storage battery) are found.

A storage battery is an energy storage device or reservoir that, when charging, directly

converts electrical energy into chemical energy. By connecting it to a consuming apparatus the stored electrical energy is recovered during discharge. The simplest operating unit is a single; several cells constitute a battery. In technical terms an electrode is a “plate”; its working constituent is the “active material”.

The positive electrode or plate of a cell is cathodic during discharge so that electrons enter it to bring about a chemical reduction. On charging an anodic reaction or oxidation occurs and the electrons leave the plate. The negative plate operates as an anode during discharge and a cathode during charge with corresponding electron exchange and chemical oxidation or reduction.

Plates of like polarity are connected in parallel either inside or outside a cell by a plate strap. Two plate assemblies with their straps, each of different polarity and their separators, form the element. The element with its electrolyte (sulfuric acid solution exclusively), cell case, cover with post, and vent cap constitute the cell unit. Cell of the same kind can be joined by connectors to form a battery.

Cells or batteries are designated by the nominal capacity in ampere hours (Ah) and by the nominal voltage, which has been standardized at 2.0V/cell for the lead acid battery. This value applies at the nominal electrolyte temperature and density.

Higher voltages are achieved by series connection of individual cells. Battery capacity is increased by using cells of greater capacity rather than parallel connection. Parallel connection of cells increases reliability somewhat, but the increase in the number of cells also increases the total battery weight.

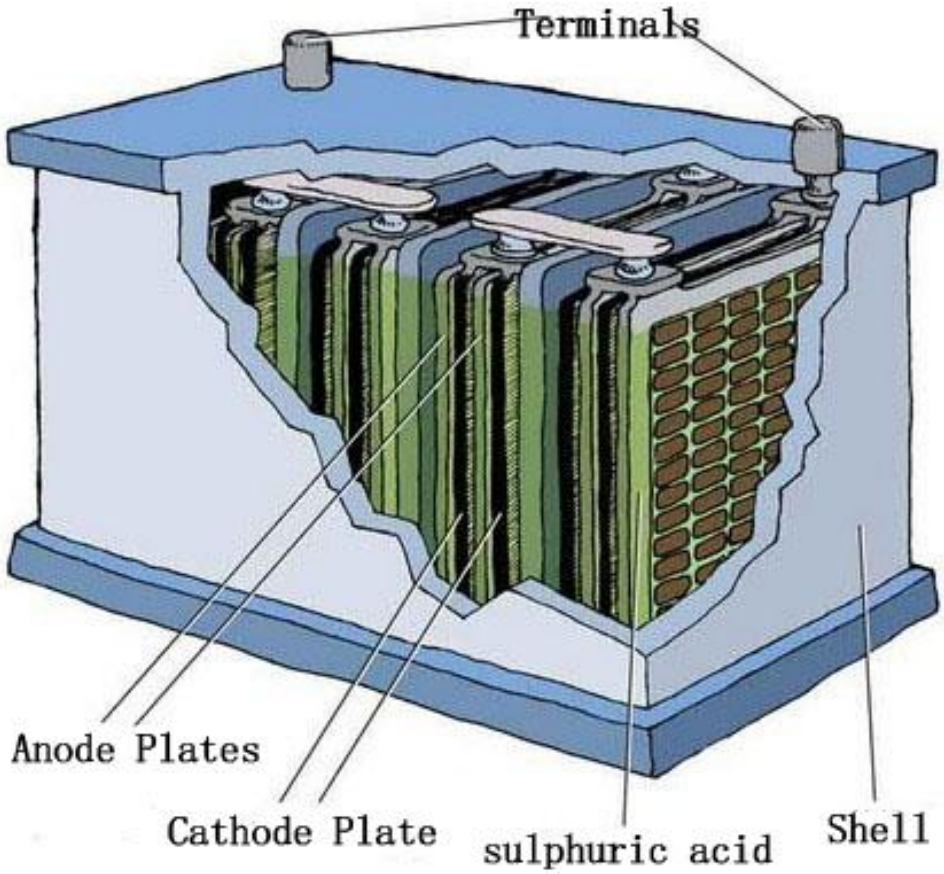

Fig 1 Structure of a lead acid battery

2.3 Advantages of AGM Battery

AGM batteries are just like flooded lead acid batteries, except the electrolyte is held in glass mats, as opposed to freely flooding the plates. Very thin glass fibers are woven into a mat to increase surface area enough to hold sufficient electrolyte on the cells for their lifetime. The fibers that compose the fine glass mat do not absorb nor are affected by the acidic electrolyte they reside in. These mats are wrung out 2-5% after being soaked in acids, prior to manufacture completion and sealing. The AGM battery can now accumulate more acid than is available, and never spill a drop.

The AGM battery used in this research is a valve-regulated, recombinant gas,

absorbed electrolyte, lead acid batteries. The cells are sealed with a pressure relief valve that prevents gases within the battery from escaping. The positive and negative plates are sandwiched between the fluid and the glass mat fibers. The mat is over 90% saturated with the electrolyte. By design it is not totally saturated with electrolyte, a portion is filled with gas. This void space provides the channels by which oxygen travels from the positive to the negative plates during charging. When the oxygen gas reaches the negative plate, it reacts with lead to form lead oxide and water. This reaction at the negative plate suppresses the generation of hydrogen that otherwise would come off the negative plate. In this manner, virtually all of the gas is "recombined" inside the cell, eliminating the need to add water, resulting in "maintenance free" operation. Furthermore, since the acid electrolyte is fully absorbed in the AGM separator, the battery will not spill even when turned upside down.

Compared to flooded-electrolyte batteries which have been in use since 1859, AGM has much lower level of self discharge rate and water loss. Though the flooded batteries are less expensive than AGM or Gel batteries, these major deficiencies cannot be simply ignored. The escape of hydrogen and oxygen from the battery represents a serious safety hazard if the gasses are not ventilated properly. Optimizations are made to reduce the amount of gassing and water loss, by replacing the antimony lead alloy with calcium lead alloy, but the cycle life is also reduced and they no longer considered deep cycle batteries. Electrolyte stratification can occur in all types of flooded batteries. As the battery is discharged and charged, the concentration of acid becomes higher at the bottom of the cell and becomes lower at the top of the cell. The low acid concentration reduces capacity at the top of the plates, and the high acid concentration accelerates corrosion at

the bottom of the plates and shortens the battery life. Although stratification can be minimized by raising the charging voltage so that the increased gassing agitates the electrolyte, this will accelerate the water loss and water refilling frequency. In addition, AGM batteries are not damaged under freezing temperatures, whereas flooded batteries will not tolerate.

As to Gel batteries, they employ a highly viscous, semisolid mixture of silica gel and dilute sulfuric acid in a colloidal suspension as an electrolyte. The electrolyte is difficult to keep homogeneous and the solid silica can separate from the acid, creating a "flooded" battery. Handling and vibration exposure are operational factors that can cause the silica and acid mixture to separate as there is no chemical bond. In high temperature environments, the semisolid electrolyte develops cracks and voids that reduce contact between the plates and causes the battery to lose capacity. By contrast, AGM batteries employ a glass micro fiber mat separator that holds the liquid electrolyte like a sponge. Shrinkage of the separator does not occur as the battery ages and the electrolyte remains in direct contact with the plates. The electrolyte spillage or leakage is prevented. There are more differences like AGM has lower sensitivity to current than Gel batteries. Impropriate current applying to Gel batteries will affect their cycle life. And to AGM type also takes shorter time to get fully charged than Gel batteries.

CHAPTER 3

CIRCUIT MODEL DEVELOPMENT

Recently large quantities of models exist, from the simplest, containing impedance placed in series with a voltage source, to the most complex. In general, these models represent the battery like an electric circuit composed of resistances, capacities and other elements, constant or variable. Function of the temperature or the state of charge gives an idea on the quantity of chemical active mass inside the battery.

The selected battery has a 12V nominal voltage and capacity of 89Ah at the 24-hour rate. The circuit model for this battery is designed by using both manufacturer's manual data and test results, because discharging the battery to a very low state of charge (SOC) level will cause damage and permanently reduce its lifecycle, which also affects the following test results of the same battery.

The SOC and depth of discharge are explained before going into further discussion. The DOD is the percentage of the discharged capacity of a battery which is fully charged before discharging.

$$DOD = \left(\frac{Q_d}{Q_{rated}}\right) \times 100\%$$

where Q_d and Q_{rated} are the discharged capacity and the rated capacity, respectively, both in Ampere-hour(Ah).

On the other hand, the SOC is defined as the percentage of the remaining capacity of a battery.

$$SOC = \left(\frac{Q_r}{Q_{rated}}\right) \times 100\%$$

In this research, the tested battery is assumed to be healthy, and once having been fully charged can deliver the rated capacity of 89Ah at a constant current rate of 24HR by neglecting the loss produced by the higher current rate during the discharging. With these assumptions, the SOC of a battery can be expressed as

$$SOC = \left(\frac{Q_{rated} - Q_d}{Q_{rated}}\right) \times 100\% = 1 - DOD$$

3.1 Circuit Model Based on Static Characteristics

The static characteristic is closely related to the battery behavior of a single cycle life. Its feature is generally shown when applying a constant current. The discharge curves given by Fig.2 show the relation between battery terminal voltage and depth of discharge (DOD).

Each curve represents a specific discharging rate, varying from 1HR to 120HR (hour-rate). All the curves start at the same initial voltage 13.2V, and we can see the higher current rate, the more the voltage drops at the very beginning of each curve. This is because of the effect of the inner resistance; the voltage is proportional to current, by Ohms law.

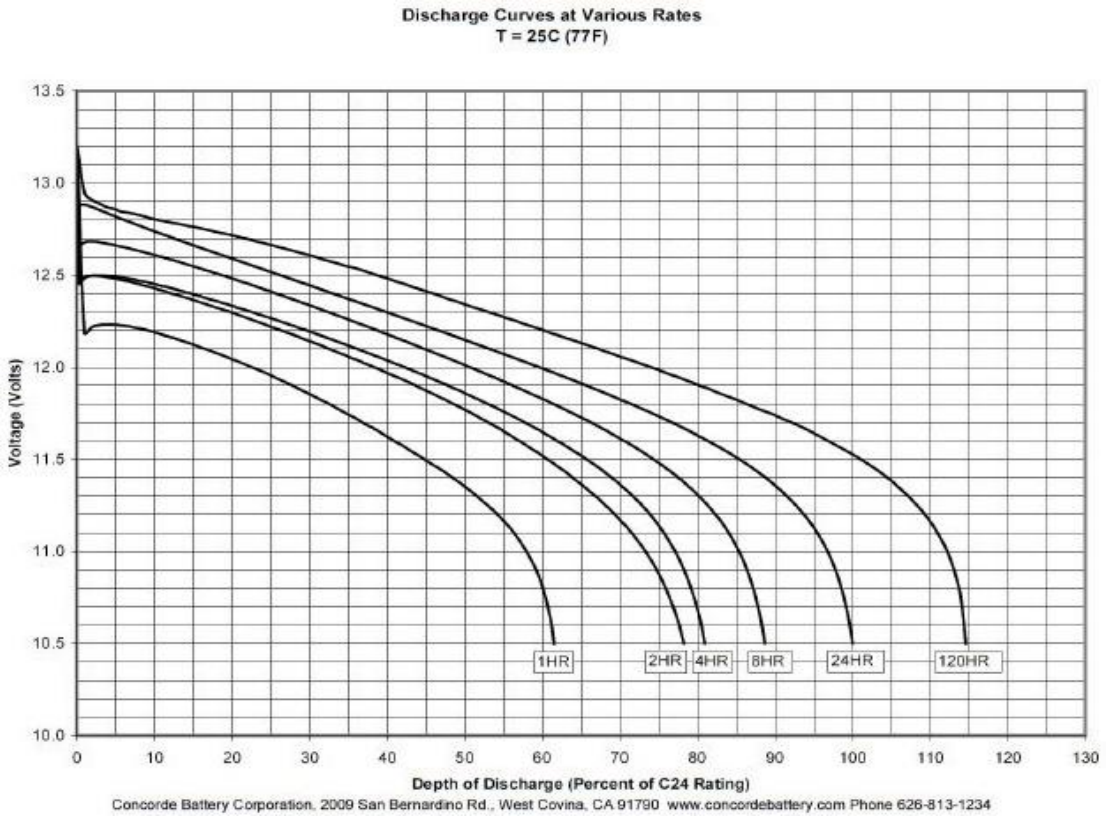

Fig 2 Manufacturer's data for discharging curves [Concorde Technical Manual]

As the DOD increases from 0 to 100%, the terminal voltage performs a sudden drop at the very beginning and then decreases at a varying slope rate. To obtain the static parameter, we first neglect the fluctuation during the switching period. A basic circuit model can be drawn to show the feature we mentioned (Fig.3),

The model contains two parts, a controlled voltage source Vs and a variable series resistor Rs. The current flowing into the battery from cathode is regarded as the positive direction. The relation between terminal voltage Vb and SOC is as the function below,

$$V_b = V_b\,(Soc) = V_s - i(t)R_s \qquad (1)$$

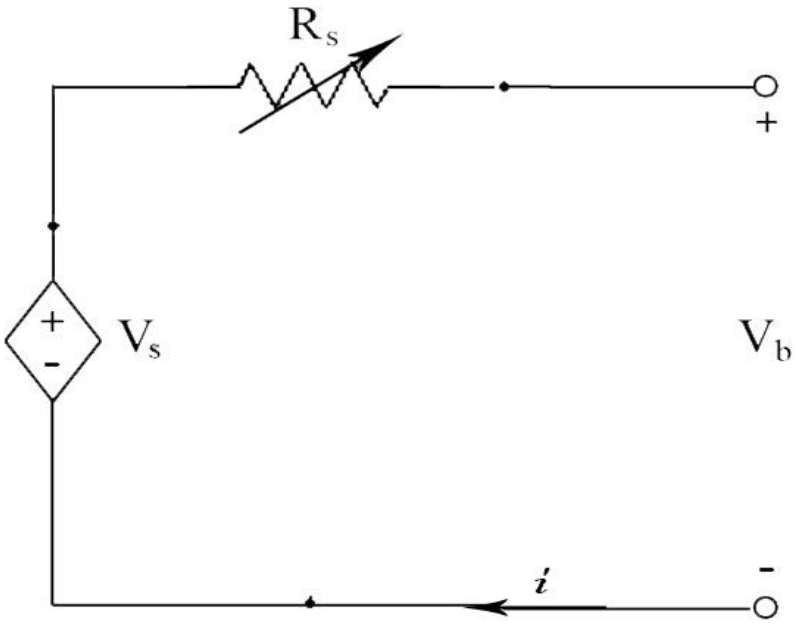

Fig 3 Equivalent circuit of the battery for static response

The SOC indicates the available capacity, ranging from 0 to 100%. It is equal to the integral of current flowing into the battery over time t, then divided by the total capacity of the battery.

$$Soc(i,t) = Soc(t_0) - \frac{\int_{t_0}^{t} i(\tau)d\tau}{3600 \times Nominal\ Capacity} \quad (2)$$

In equation (2), i(t) is the current flowing into the battery at time t, which will be negative for charging. SOC(t_0) is the initial state of charge. The nominal capacity of this model is 89Ah. In this case, the equation of SOC can be rewrite into as the following.

$$Soc(I,t) = Soc(t_0) - \frac{It}{3600 \times 89Ah} \quad (3)$$

Vs is the voltage directly generated by the internal chemical components, the effect of this voltage source could be replaced by an equivalent capacitor Cs.

From the basic definition of capacitor, Vs can be written into the following expression,

$$Vs = Vs(t_0) - \frac{1}{Cs}\int_{t_0}^{t} i(\tau)d\tau \tag{4}$$

noticing that the capacitance Cs is also a non-linear function of SOC. $Vs(t_0)$ is a constant number indicating the initial voltage at time t0.

So the terminal voltage Vb is written into,

$$V_b(i, Soc) = Vs(t_0) - \frac{1}{C_S}\int_{t_0}^{t} i(\tau)d\tau - i(t)\,R_s \tag{5}$$

After comparing the curves at different discharge current rate, it can be found that the Rs is only affected by the discharge current I (current is constant for each rate), so

$$V_b(I, Soc) = Vs(t_0) - \frac{It}{C_s(I,Soc)} - IR_s(I) \tag{6}$$

Equation (6) gives out the relation between terminal voltage Vb and its two variables I and SOC, the next step is to determine the expression for C_S and R_S.

Let's consider one curve in Fig.2. We can see that the curve drops more and more quickly as the DOD increases. In mathematics, an inversely proportional function can describe this feature. Meanwhile, considering that the curve has a certain slope rate from the start, there should be also a linear function in the expression of the curve.

Now we can assume that the curve is combined with two functions, one inverse-proportional and one linear.

$$V_{b1} = p\omega x + \frac{q_1 \omega x}{q_2(\omega x - q_2)} + Vs(t_0) - IR_s \quad (7)$$

where x is DOD, p, q1, q2 are parameters of the two assumed function.

Obviously equation (7) is actually another form of equation (6). Now by substituting the ordinates of the curves in Fig.1, we can figure out the parameters of equation (7) as follows:

p = -1.19;

q_1 = 0.076;

q_2 = 1.06;

$Vs(t_0)$ = 13.2 V (initial voltage)

ω=0.0117x+0.9565

Let V_b=V_{b1}. C_S and R_S now can be finally derived:

$$R_s(I) = aI^{-b}$$

$$C_s(I, Soc) = \frac{AH \times 3600}{p \times (cI+d) - \frac{q_1 \times (cI+d)}{q_2 \times (cI+d)(1-Soc) - {q_2}^2}}$$

Table.1 Parameter value for the expressions of C_S and R_S

Parameters	a	B	c	d	p	q1	q2
Value	0.275	-0.704	0.012	0.957	-1.190	0.076	1.060

AH is the capacity of the battery

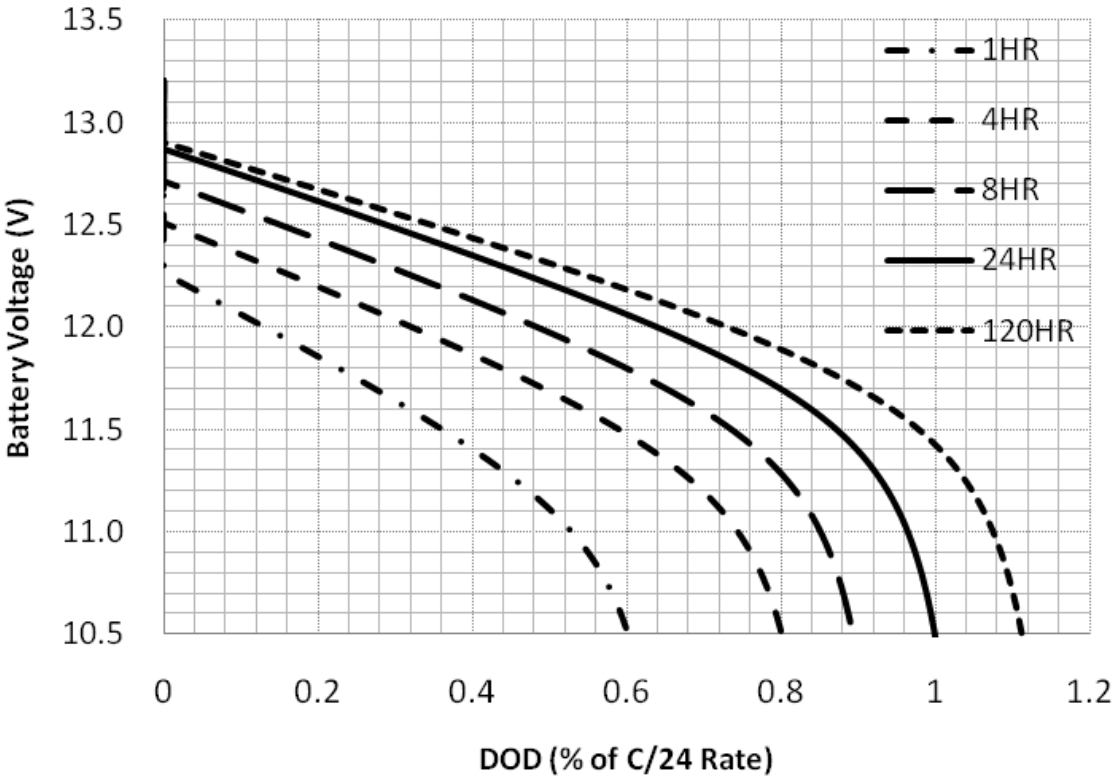

Fig 4 Curves of the battery function, different discharge rates, comparing to Fig.2

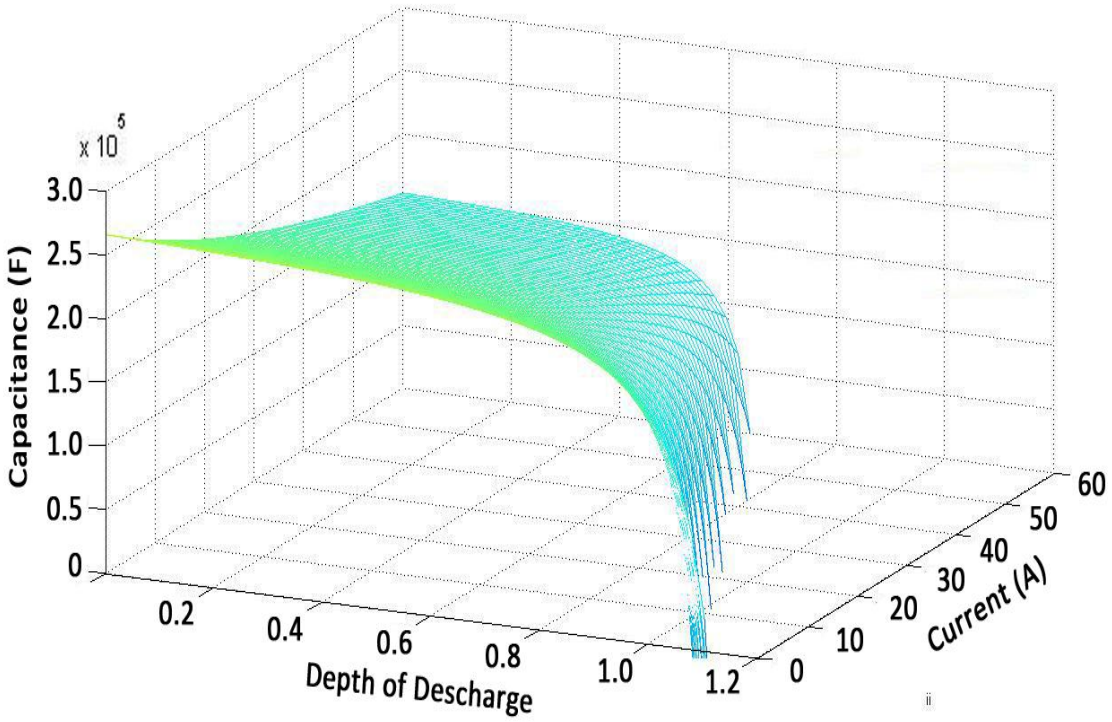

Fig 5 Equivalent capacitance is a function of I (0~60) and DOD (0~1.2)

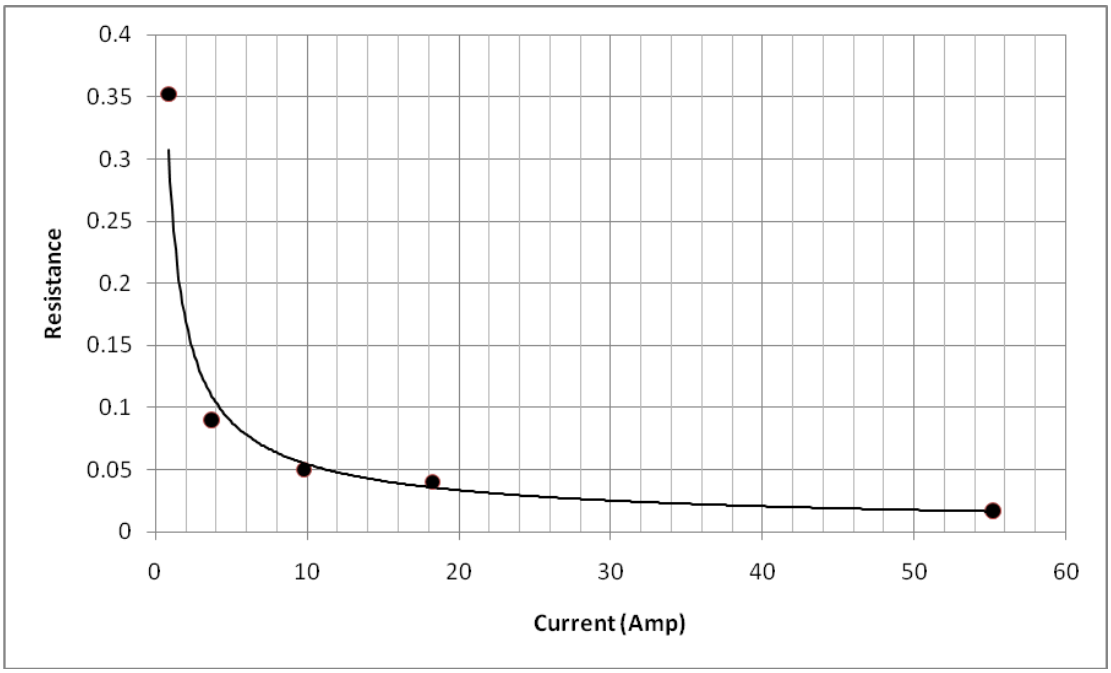

Fig 6 R_s is a function of current according to manufacturer's data

3.2 Circuit Model Based on Dynamic Characteristics

The dynamic response of the battery is affected by the transient parameters, which could be represented by an internal RC circuit. Starting with the model developed, we split the series resistor Rs into two parts, letting one of it be in parallel with a capacitor, which is Rt. The remained part of Rs stays in series:

$$Rs = Rs' + Rt \tag{8}$$

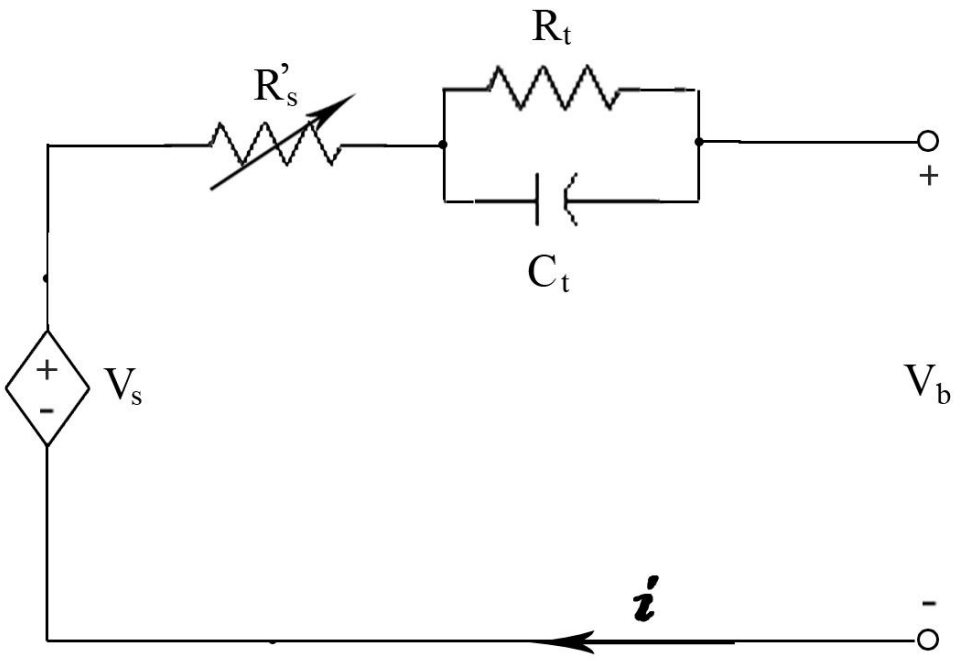

Fig 7 Equivalent circuit for dynamic response

The voltage variation on R_s' and R_t is described by the following equation:

$$V_{drop} = -IR_s^{'} - IR_t\left(1 - e^{-\frac{t}{R_tC_t}}\right) - V_c e^{-\frac{t}{R_tC_t}} \quad (9)$$

where V_c is initial voltage stored in capacitor C_t. Both of R_s' and R_t could be either a function of current I or a constant. Time t is already defined in equation (3) and can be easily written into the function of SOC. R_tC_t is the time constant of the RC circuit.

Now replace the voltage variation in equation (6), we obtain the battery function based on both static and dynamic parameters:

$$V_b(I, Soc) = Vs(t_0) - \frac{It}{C_s(I, Soc)} - IR_s^{'} - IR_t\left(1 - e^{-\frac{t}{R_tC_t}}\right) - V_c e^{-\frac{t}{R_tC_t}} \quad (10)$$

Since the resistor R_s is split into two parts, the expression of R_s derived from equation (6) and equation (7) will probably be no longer suitable. New expression for R_s may include both expressions for R_s' and R_t. The manufacturer's data doesn't indicate these two variables. Lab experiments need be carried out for determining their values.

CHAPTER 4

TEST SYSTEM AND PROCEDURE

This test system contains the test battery, an auto-charger, a configurable load bank , a data logger and several resistors. The battery is a 12V, 89Ah AGM. All the tests are in room temperature (17 – 25 degree Celsius). Fig.8 shows the equipment and its connections.

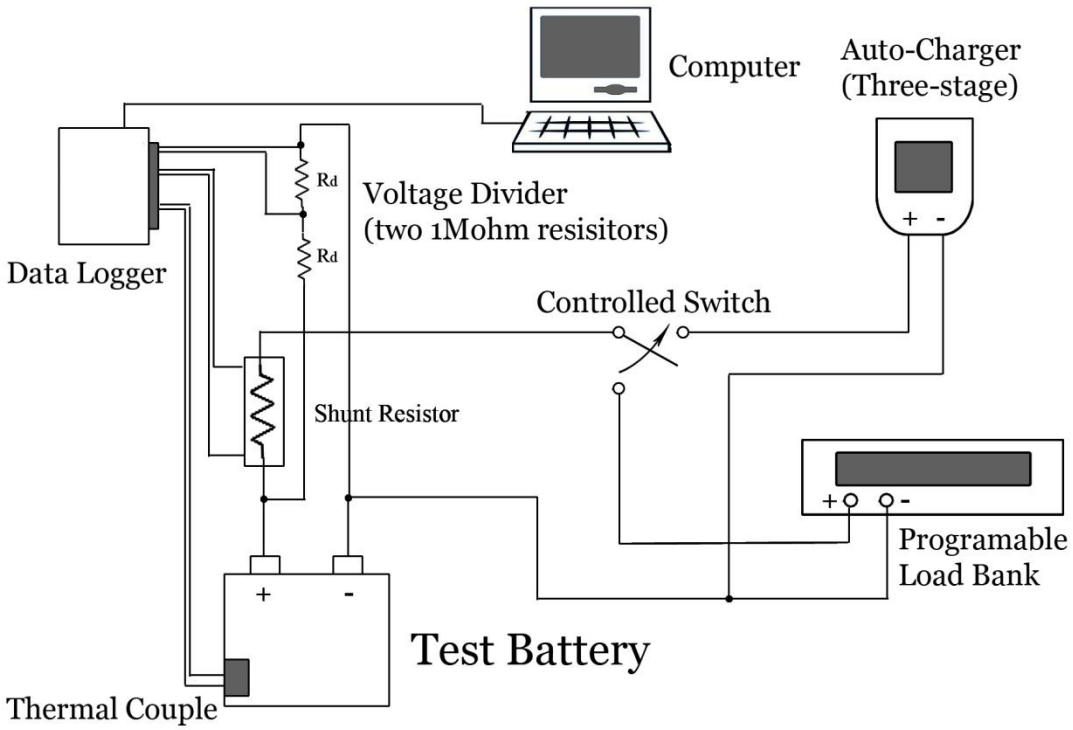

Fig 8 Schematic Diagram of Test System

4.1 Test Equipments

Test Battery:

The PVX-890T battery contains 6 cells. Each of them provides 2V output voltage in

general. Two copper alloy terminals are designed for corrosion resistance and high conductivity. The cover or container is made of reinforced poly propylene to be a perfect insulator.

Fig 9 Sun Xtender PVX-890T AGM battery

The AGM battery is designed to reduce the amount of released hydrogen and oxygen gas, however, for safety consideration, good ventilation is also designed during charging procedure. The battery is located at the open place of the room and a fan is used to keep the flow of air around the battery.

Charger:

The charger will apply the three-stage charging sequence using 20A input current. The voltage and current are pre-programmed and cannot be adjusted during the test. The charger itself will detect the battery output voltage and complete the stage switches automatically. There is an option button for in AGM battery particularly, to chose between 2-stage and 3-stage charging. The option for environment temperature is

selected to be “warm”.

Fig 10 Xantrex Auto Charger with 20A input current

Load Bank:

This DC load is a two terminal device that can be connected to DC sources. It can draw a constant voltage, a constant current, a constant power from a DC source and can present a constant resistance to the DC source. The current can be configured as precisely as to 0.001A.

The load bank is responsible for discharge test. The two terminals are connected to the anode and cathode of the battery. Because of the inaccuracy of the data logger, the voltage measured by this load bank is selected to be a standard value, the results of recorded by the data logger need to be modified. The correction factor is given in the paragraph for introduction of the data logger. The load bank has a 300W nominal power, so the current flowing into it should not be higher than 25A, as a limitation.

Fig 11 The programmable DC electronic load

Shunt Resistor:

A shunt resistor Rg is implemented in series to record current by measuring the voltage across it. Rg is quite sensitive and with low inaccuracy, its 100mΩ impedance gives an output of 1 mV when there is 1A through it.

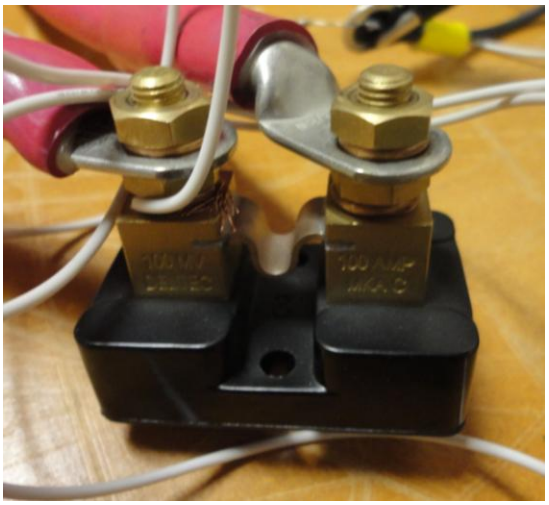

Fig 12 High accuracy shunt resistor

Data Logger:

The data logger OM-DAQPRO-5300 is an eight-channel portable data acquisition and logging system with graphic and build-in analysis functions. The eight input channels are for measuring voltage, current, temperature and pulses. Selectable ranges for each input are 0-24mA, 0-50mA, 0-10V, a large variety of NTC thermistors, PT-100 RTDs and thermocouple temperature sensors including internal temperature, pulse counter, frequency meter and up to 20 user defined sensors. The inputs use pluggable screw terminal blocks for easy connection.

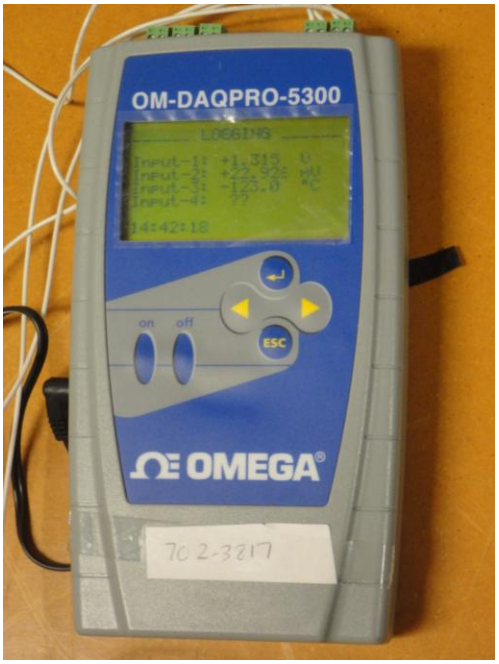

Fig 13 OM-DAQPRO-5300 Data Logger

Considering the voltage range of the data logger is lower than the battery voltage, a voltage divider is applied by using two 1MΩ resistors R_d. The data logger measures the voltage across one of them. However, the voltage across the resistor is not simply half of the battery voltage. The internal resistance of the data logger itself R_{data} must be taken to

account:

$$V_{data} = V_b \times \frac{R'}{R_{total}} = V_b \times \frac{\frac{R_d R_{data}}{R_d + R_{data}}}{R_d + \frac{R_d R_{data}}{R_d + R_{data}}} \quad (11)$$

where R_d=1MΩ and R_{data}≈125Ω.

From equation (11) the relation between voltage V_{data} and V_b can be found, which is $V_{data} = 0.1V_b$. The values measured by the data logger are only 1/10 of the battery voltage. This number is convenient for data recording and future calculations. In addition, the numbers obtained by the data logger cannot put into use before correction. During the test we noticed that the current into the data logger is the main reason of inaccuracy. High current brings greater errors. After comparing the results of both the data logger and load bank from an examining circuit, all the voltage values from the data logger can be corrected by the following formula:

$$V_{data.corrected} = V_{data} - (|I_{data} - I_{standard}|) \times 0.2$$

4.2 Test Procedure

The test procedure includes an overnight discharge, a long term discharge using 4HR(18.25A) and 8HR(9.8A) rates to obtain a overall discharge curve, a three-state charging sequence to obtain the behavior of the battery during recharging, several short term discharges to get the transient responses in order to figure out the value of the

elements in the RC part and a current step sequence test to verify the transient parameter obtained by the pulse discharge.

The tests are arranged in the following sequence:

1. Overnight self discharge
2. 5-min short current pulse discharge
3. Long-term constant current discharge
4. Step current sequence discharge
5. Non-uniform discharge test

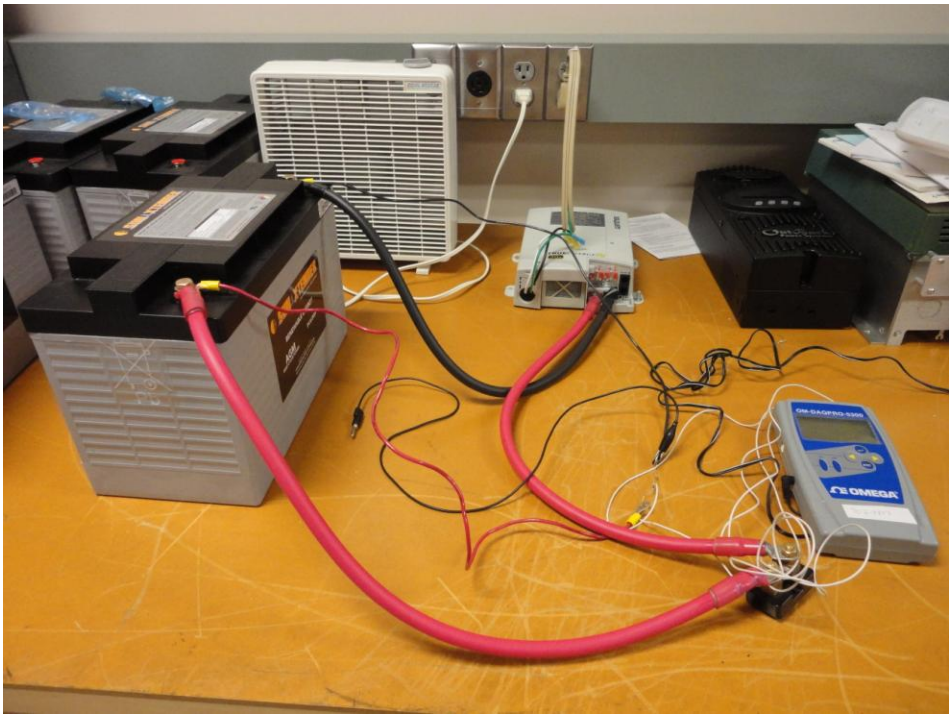

Fig 14 Connection for charging procedure

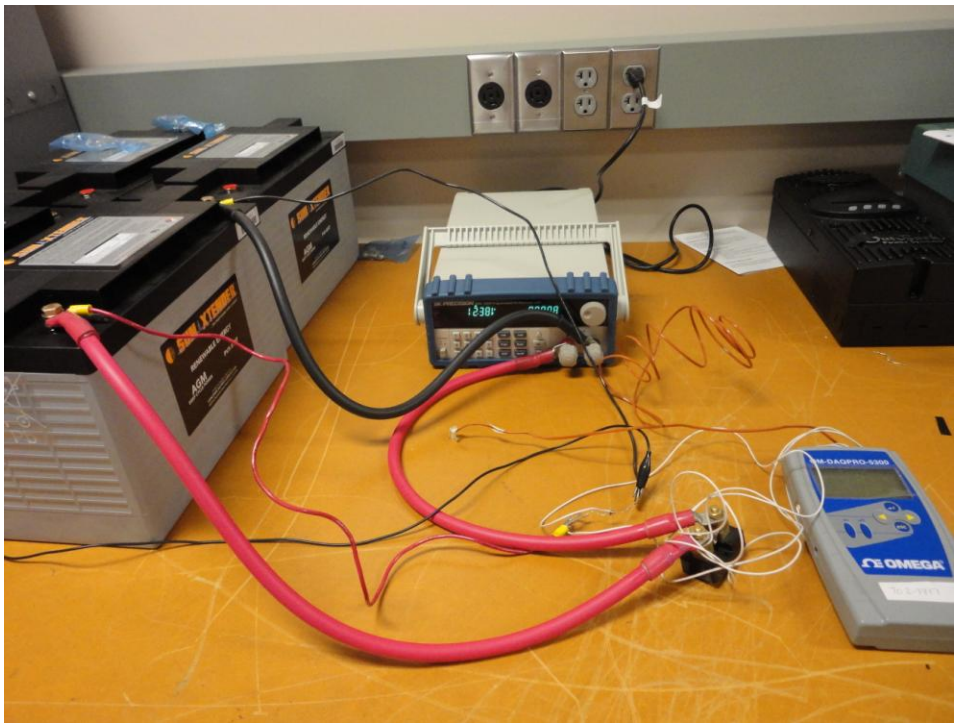

Fig 15 Connection for discharge procedure

CHAPTER 5

TEST RESULTS AND MODEL VALIDATION

5.1 Task 1: Overnight Self-discharge

After the battery is fully charged, the open circuit voltage will approach 13.2V which is used as the starting voltage in Fig.1. However, in a real situation this value doesn't last for long; it will actually drop quickly at the very beginning, decreasing by 0.1V within the first one minute. So the purpose of this test is to find the correct open circuit voltage for this fully charged battery.

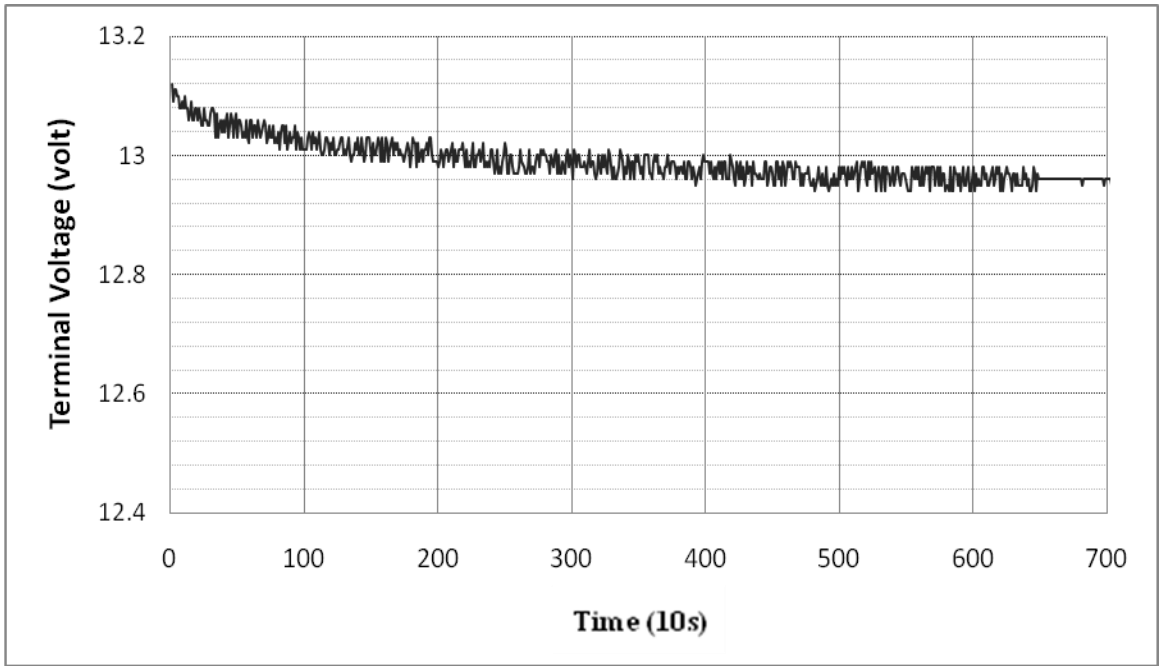

Fig 16 Test result of overnight discharge, unit for x-axis is 10 seconds

In Fig.16 we can see that after about 13 hours of "rest", the voltage drops from 13.13V to 12.95V and almost gets stable. This phenomenon is mainly caused by the charges accumulated at the terminals after using; it is hard to get the accurate result until most of these charges dissipate. The starting voltage for this particular fully charged

battery is around 12.95V or lower.

5.2 Task 2: 5 Minutes Short-term Discharge Using Different Rates of Current Pulse

The short-term discharge applies 20A, 15A, 10A and 5A current pulse. Each of them lasts 5 minutes to ensure the capacitor C_t is charged to the value of IR_t. After that the battery will be disconnected from the load for about 10 minutes to wait battery voltage go back to the starting voltage. During each pulse, Rs' can be found by evaluating every direct jumps of voltage, Rt and Ct can be found by fitting the exponential zone with an exponential function.

This procedure also tested different starting voltages (12.94v, 12.66v, 12.46v and 12.22v), which indicates the different SOC of the battery. In this step of the test, we assume that the selected current pulses will not affect the SOC since the duration of each pulse is so short comparing to the hours long, entire discharging process, which means in short-term discharge test, every time when current falls to zero, the voltage will go back to the starting voltage based on a certain time constant R_tC_t.

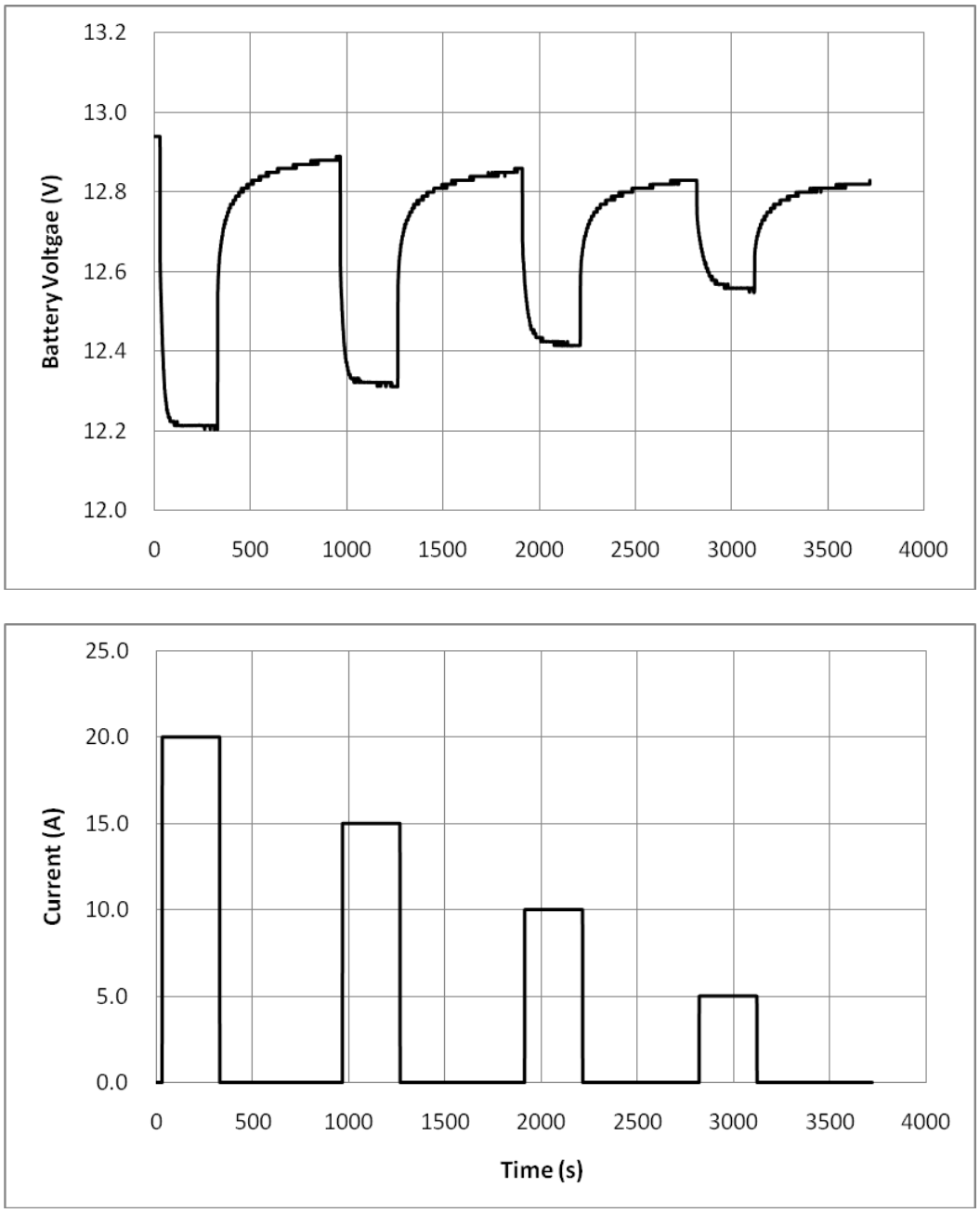

Fig 17 Pulse discharge starting at 12.94V

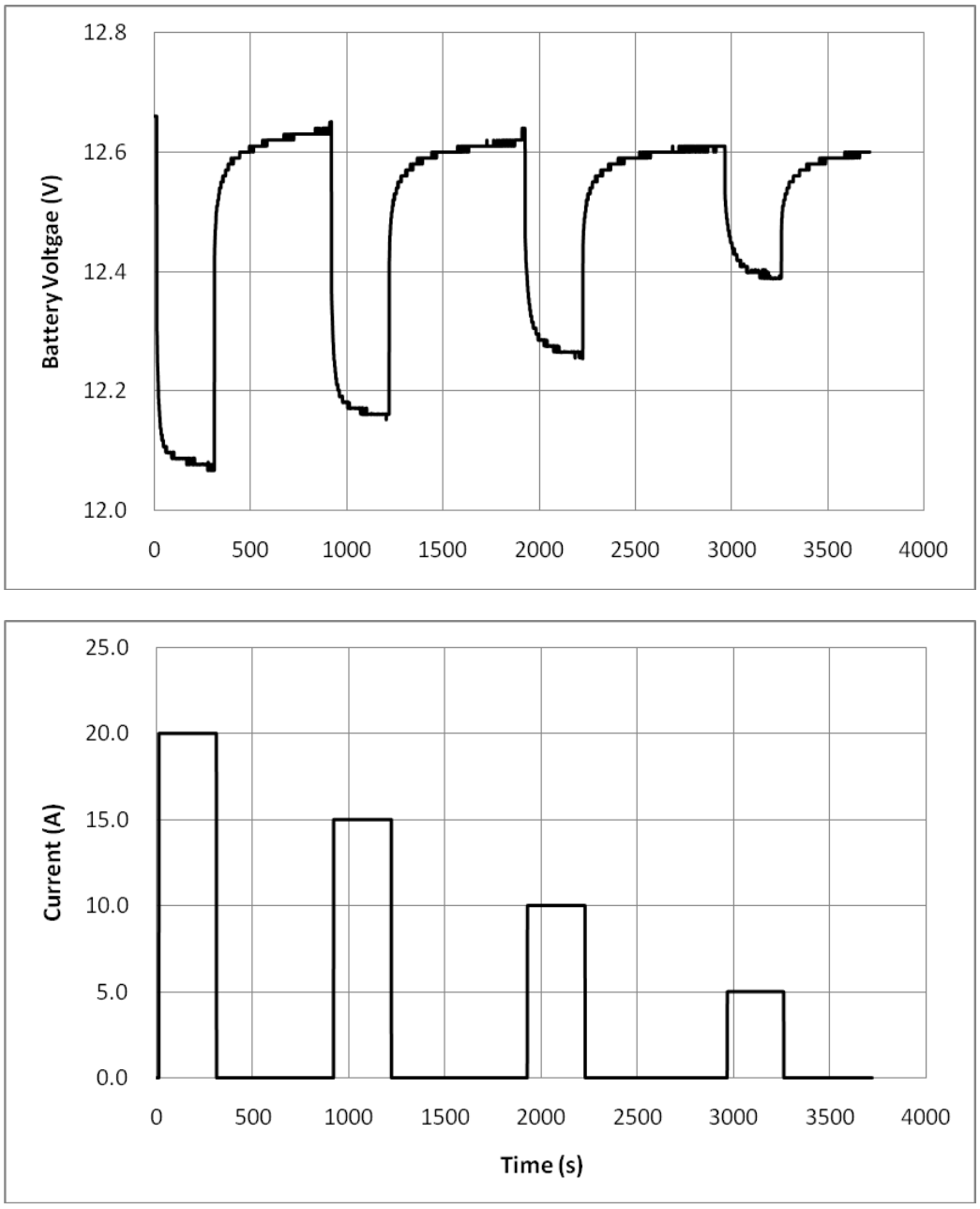

Fig 18 Pulse discharge starting at 12.66V

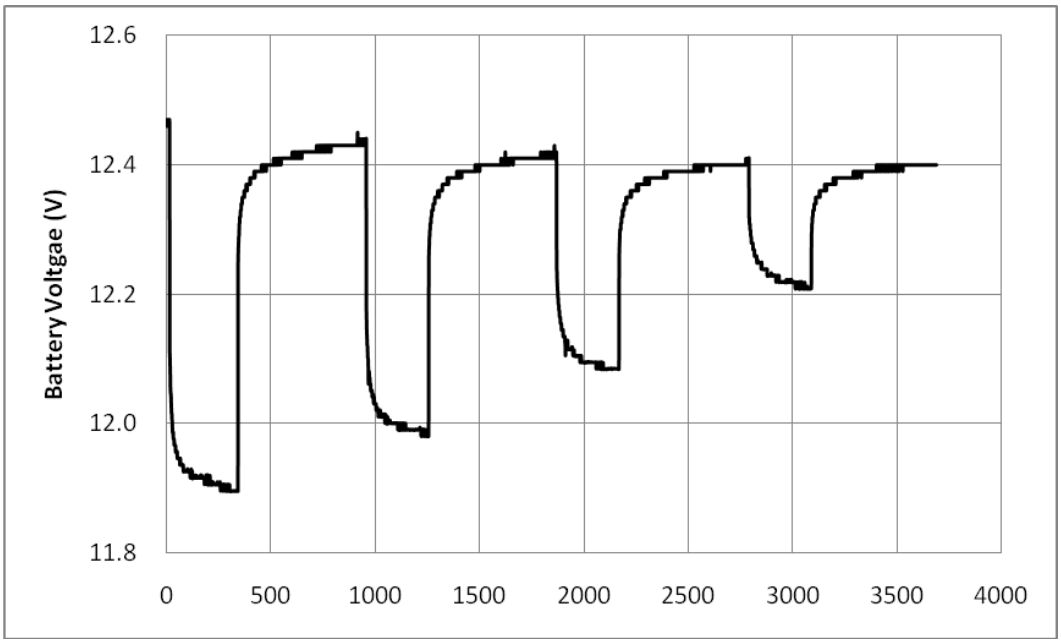

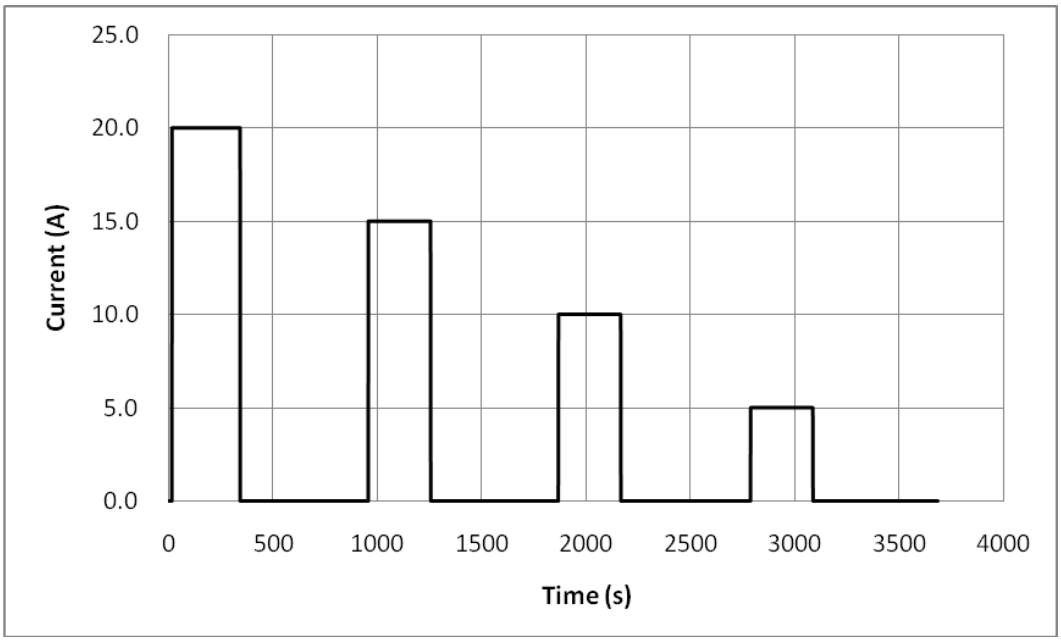

Fig 19 Pulse discharge starting at 12.46V

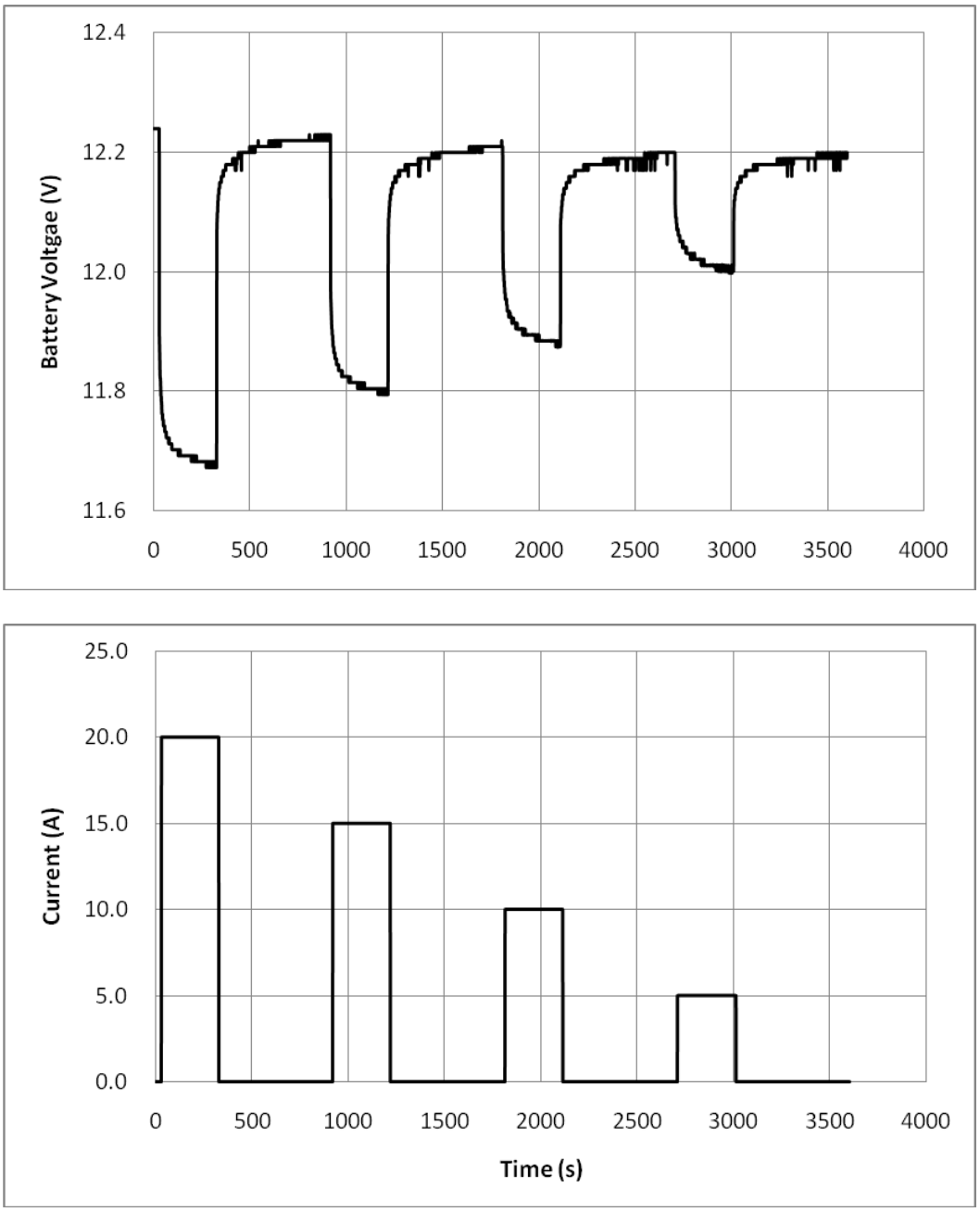

Fig 20 Pulse discharge starting at 12.22V

The plots in Fig.17 to Fig.20 clearly show that for every current pulse, the corresponding voltage changes in a similar way. The direct jumps are the vertical parts at the beginning and end of the pulses in each picture. By measuring the length of these vertical parts, we can estimate the voltage drop on a series resistor, which is Rs'. On the other hand, the voltage behaviors in the pulse duration and the rest period are typical zero input response of a RC circuit.

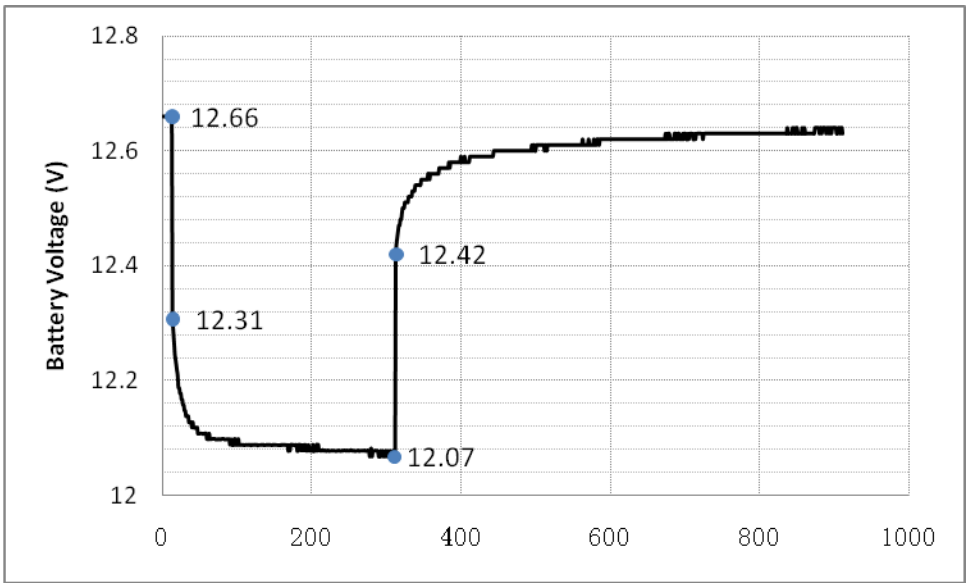

Fig 21 Extract coordinates for calculation from each current pulse's duration

By gathering the coordinates of several points on the curve, the time constant R_tC_t can be calculated by employing the basic function for RC in electric circuit theory. The transient resistance R_t can be found by measuring the voltage difference between the starting voltage and voltage value at the end of each pulse. This amount is the voltage drop on R_t; it doesn't change instantly because of the capacitor in parallel.

The results are shown by Table.2. We can see that R_s' doesn't change much with different current and starting voltage. R_t decreases with a higher current and with a lower

battery voltage.

The time constant R_tC_t also seems to be a constant. The error of the test is mainly because of the minimum step of the data logger is one second, which is not accurate enough to show the exact voltage changes at the transients. Tests with more accurate equipment will reduce this error.

Table.2 Evaluation results for dynamic parameters

Voltage Parameters		12.94v SOC:100%	12.66v SOC:83%	12.46v SOC:76%	12.22v SOC:49%
R_s' (ohms)	20A	0.0182	0.0171	0.0175	0.0177
	15A	0.0179	0.0177	0.0172	0.0168
	10A	0.0175	0.0180	0.0179	0.0181
	5A	0.0167	0.0169	0.0177	0.0177
R_t (ohms)	20A	0.0191	0.0121	0.0114	0.0082
	15A	0.0212	0.0157	0.0146	0.0112
	10A	0.0252	0.0183	0.0176	0.0121
	5A	0.0281	0.0244	0.0237	0.0211
R_tC_t (sec)	20A	11.77	14.19	12.85	13.41
	15A	11.23	14.46	12.83	11.44
	10A	12.87	11.08	12.60	11.34
	5A	12.20	10.06	14.00	14.20

From Table.2, The parameters are derived as the following table:

Table.3 Calculated dynamic parameters

Parameters	Value
R_s	$R_s'+R_t$
R_s'	0.0175 ohms
R_t	$0.0489\ e^{-0.147I} + 0.0171SOC-0.00275$
R_tC_t	12

5.3 Task 3: Step current sequence discharge

The step current sequence is applied for the purpose of model verification. The dynamic parameters obtained by simple current pulses are now applied into more complex condition. The step current sequence is a combination of four current pulses, with the same value (20A, 15A, 10A, 5A) and length (5 minutes) as the pulses used in the previous test but no rest period between one another. That means after each pulse, the capacitor has no time to release the charges to zero. Meanwhile, the change of the current resets the final voltage of the capacitor. The capacitor will keep obtaining or release charges to get the adjusted voltage. During this process, the accuracy of the parameters can be examined.

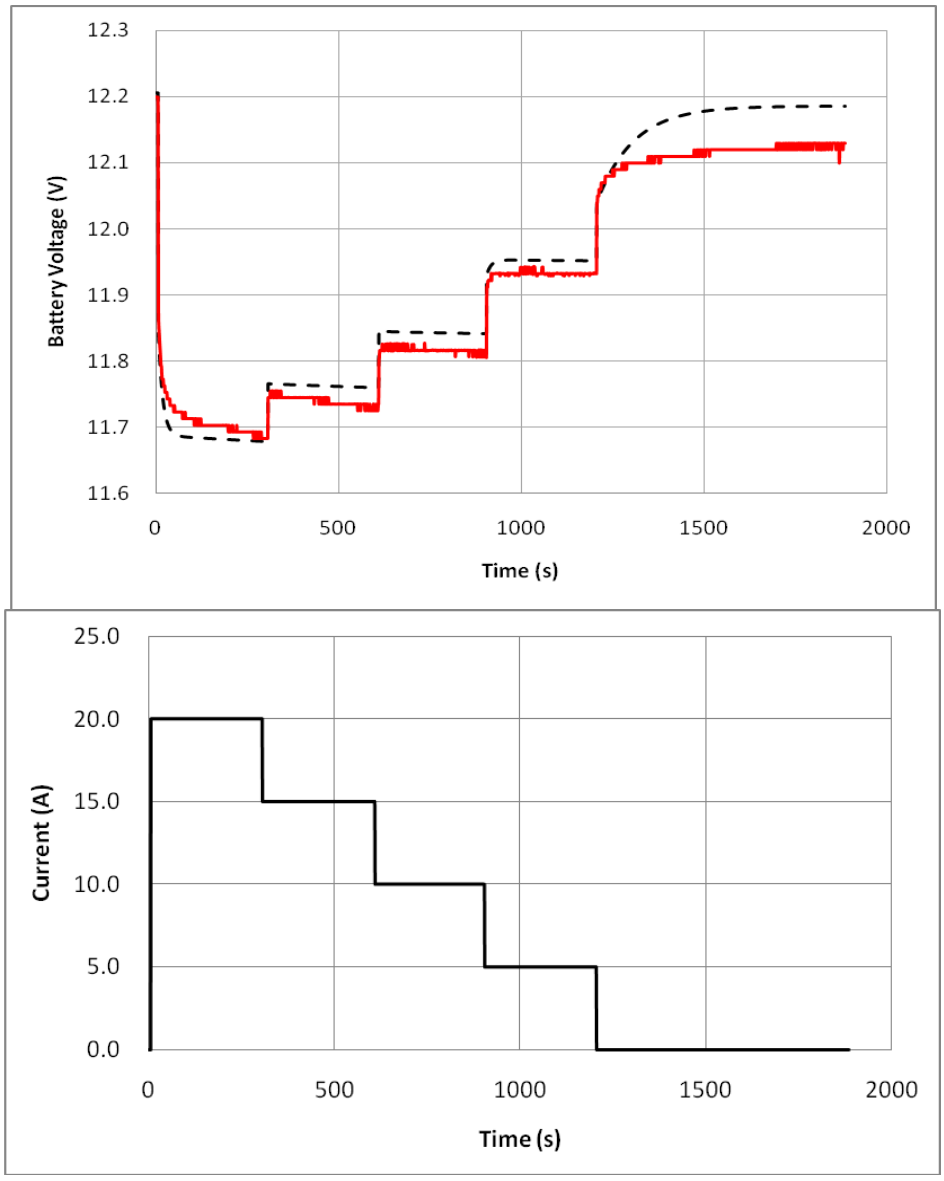

Fig 22 Results of step current sequence (20A-5A)

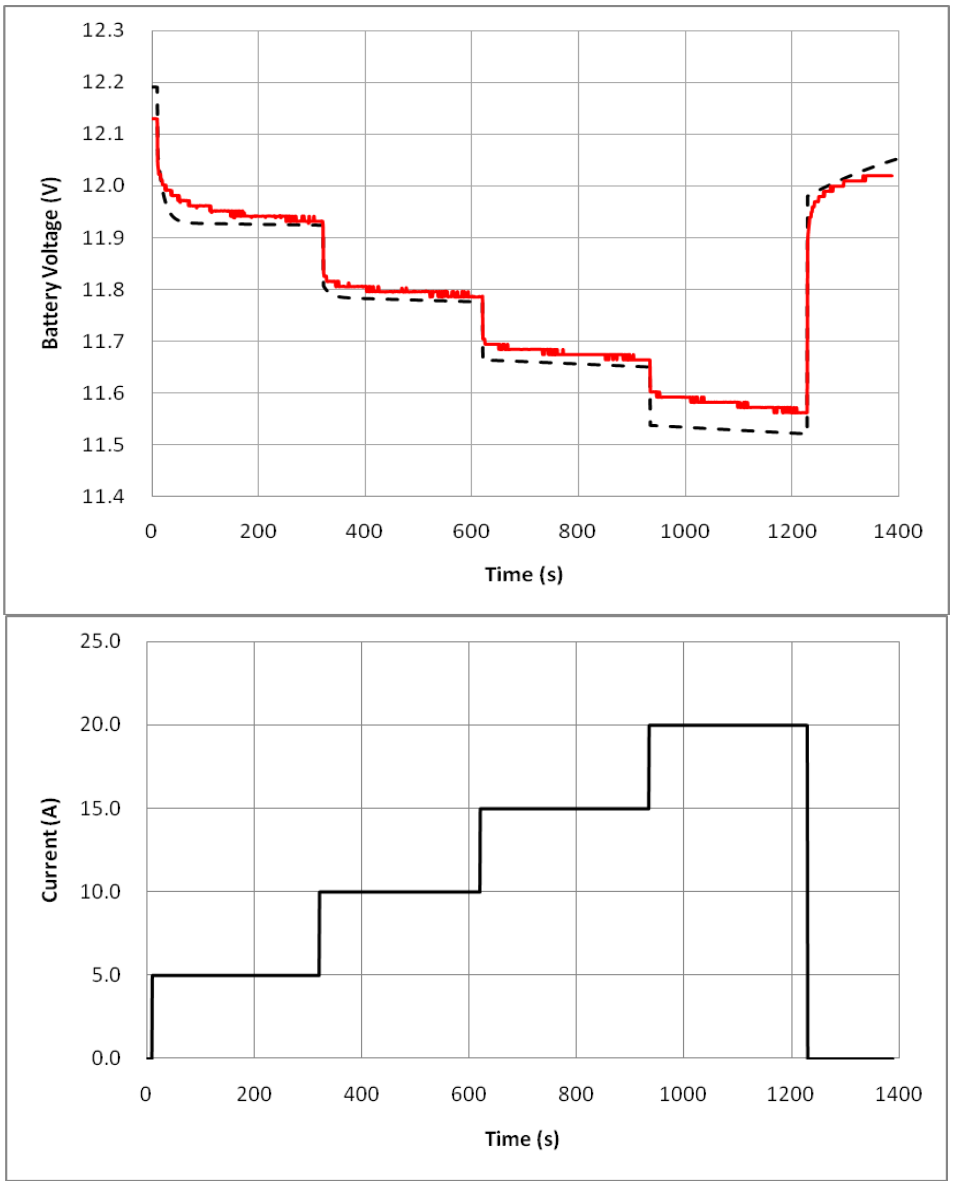

Fig 23 Results of step current sequence (20A-5A)

5.4 Task 4: Non-uniform current discharge

The results of applying step current sequence are very good. The model curve behaves close to the battery curve. Now a non-uniform current sequence is applied to both the battery and the circuit model again.

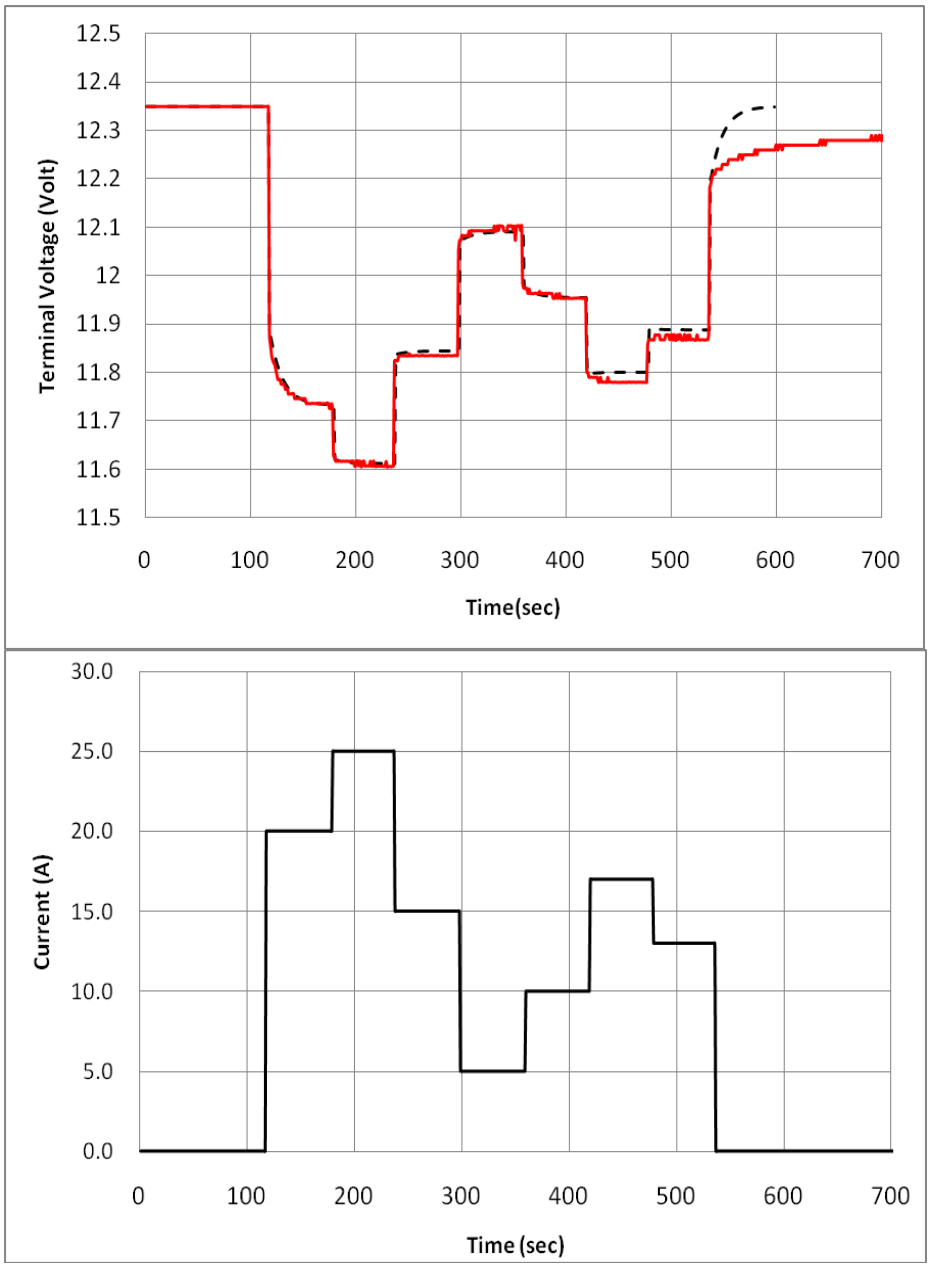

Fig 24 Voltage response of a non-uniform current sequence

The current sequence is pre-set but the values of each pulse are randomly picked. The duration of each step is 60 seconds, current changes from one value to another without any rest period, which is so short that the capacitor is hard to get settled with the new voltage value. Applying a more complex condition like will give better result for model validation.

Fig.24 gives a clear picture that how the model simulation results (dashed line) fits the experimental data (solid line). We can see that except for the final part, the model follows very closely to the battery behavior, which means this model is acceptable. The error of this test is 1.49%. The mismatch in the last part may be caused by the property of the active mass in the battery. Its time constant seems to become extremely large after the current drop to zero.

5.5 Task 5: Long-term discharge at 4HR(18.25A) and 8HR(9.8A) rates

After determine the dynamic parameters, the total internal resistance is obtained. In another way, the voltage drop in the steady discharge can be calculated. This long-term discharge is to validate the static response of the model. In chapter 3, the circuit model is derived from the manufacturer's voltage curve data. After that, the model is further updated and modified. Now two tests are carried out to show how the model fits the real battery. Two current rates are picked for this test, 4HR and 8HR, whose results can be compared with the plots in Fig.4. No higher current is tested considering the nominal power of the load bank.

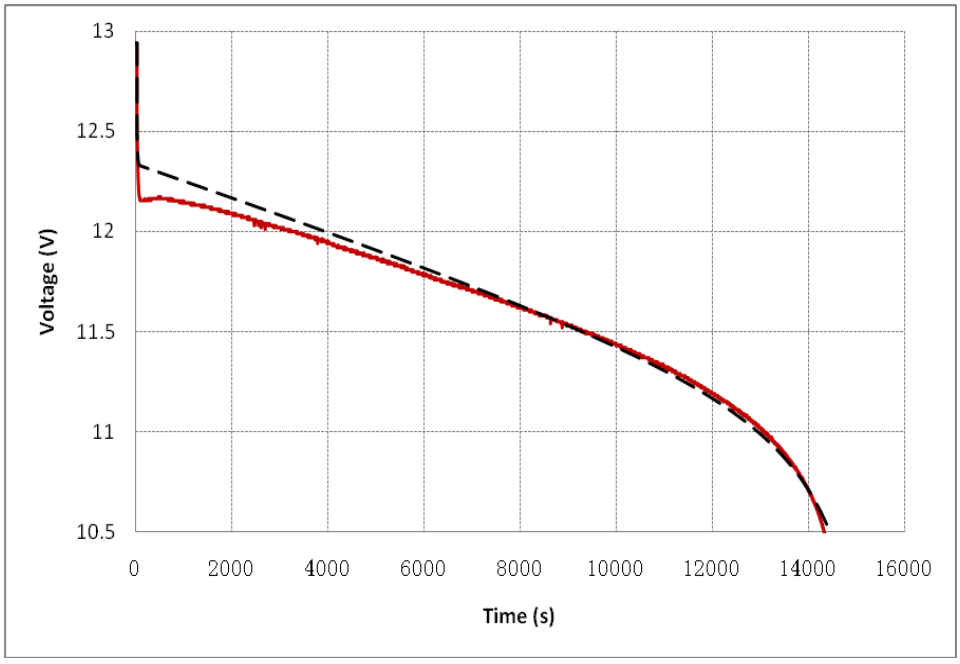

Fig 25 Results of long-term discharge using 18.25A constant current (voltage versus time)

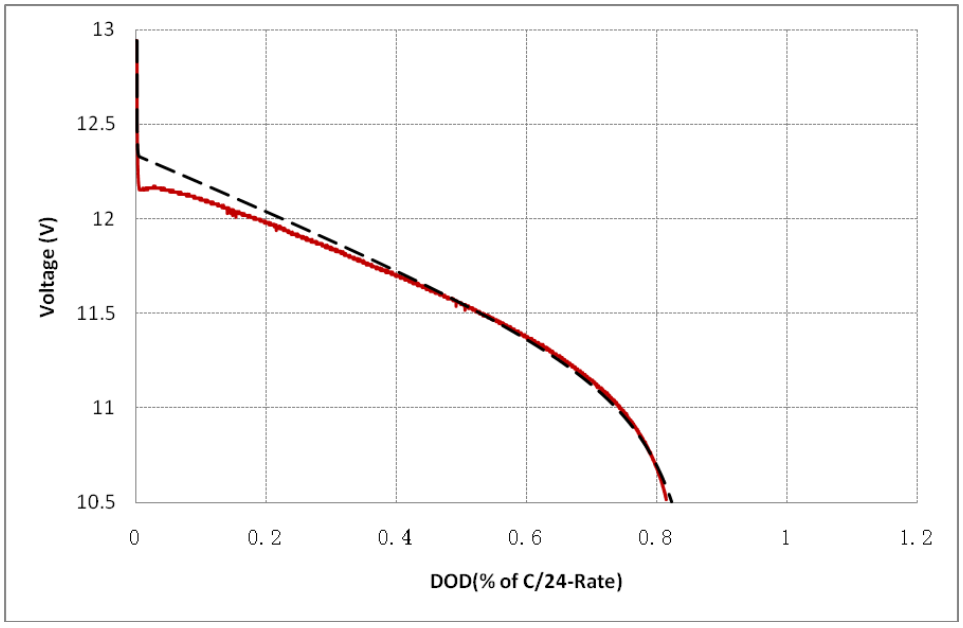

Fig 26 Results of long-term discharge using 18.25A constant current (voltage versus DOD)

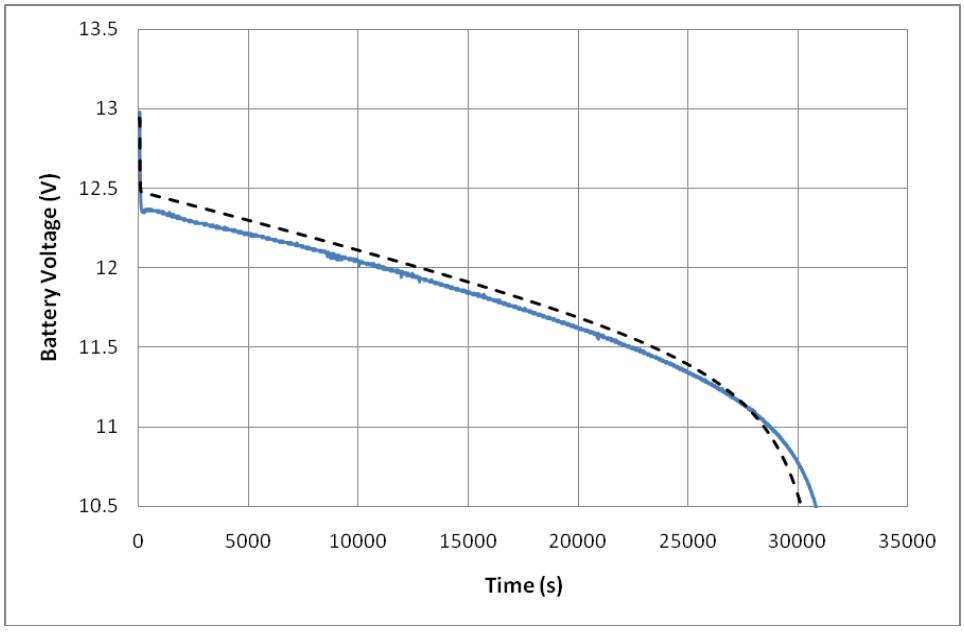

Fig 27 Results of long-term discharge using 9.8A constant current(voltage versus time)

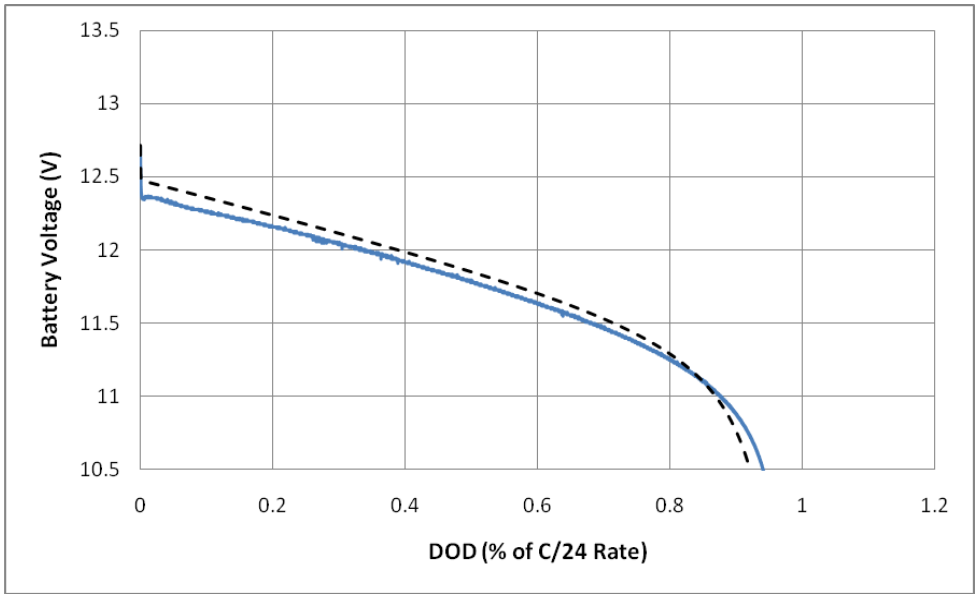

Fig 28 Results of long-term discharge using 9.8A constant current(voltage versus DOD)

In Fig.25 and 27, the solid lines stand for the experiment data and dashed lines are for the proposed model. The result of using 4HR rate is closer to the test data than using 8HR rate. Both of these two results are in acceptable error range. The error for using 4HR is 0.54% and for using 8HR is 1.16%.

A long term discharge at half of the battery cycle life is also tested. As shown in Fig 29, the two curves match perfectly. The reason for this result is because the disappearance of the voltage dip that caused by the polarization effect, which only occurs when the battery start discharging at about 100% SOC using a high rate of current.

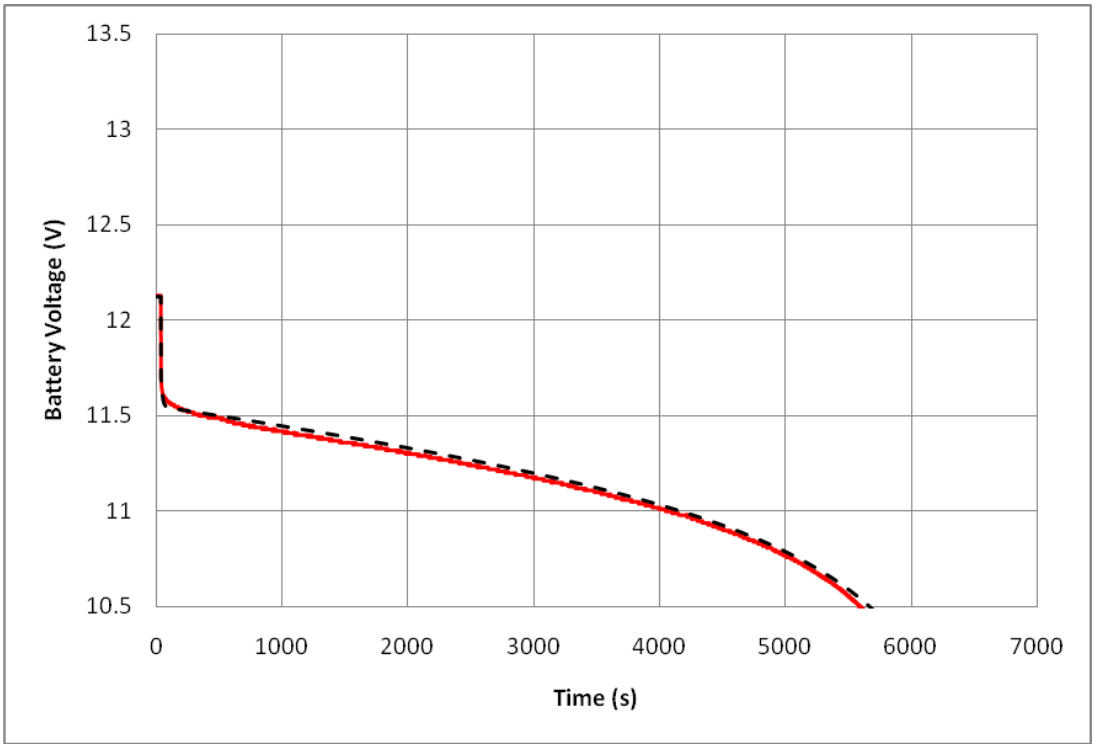

Fig 29 Discharge of the battery from 50% of SOC (Voltage versus time)

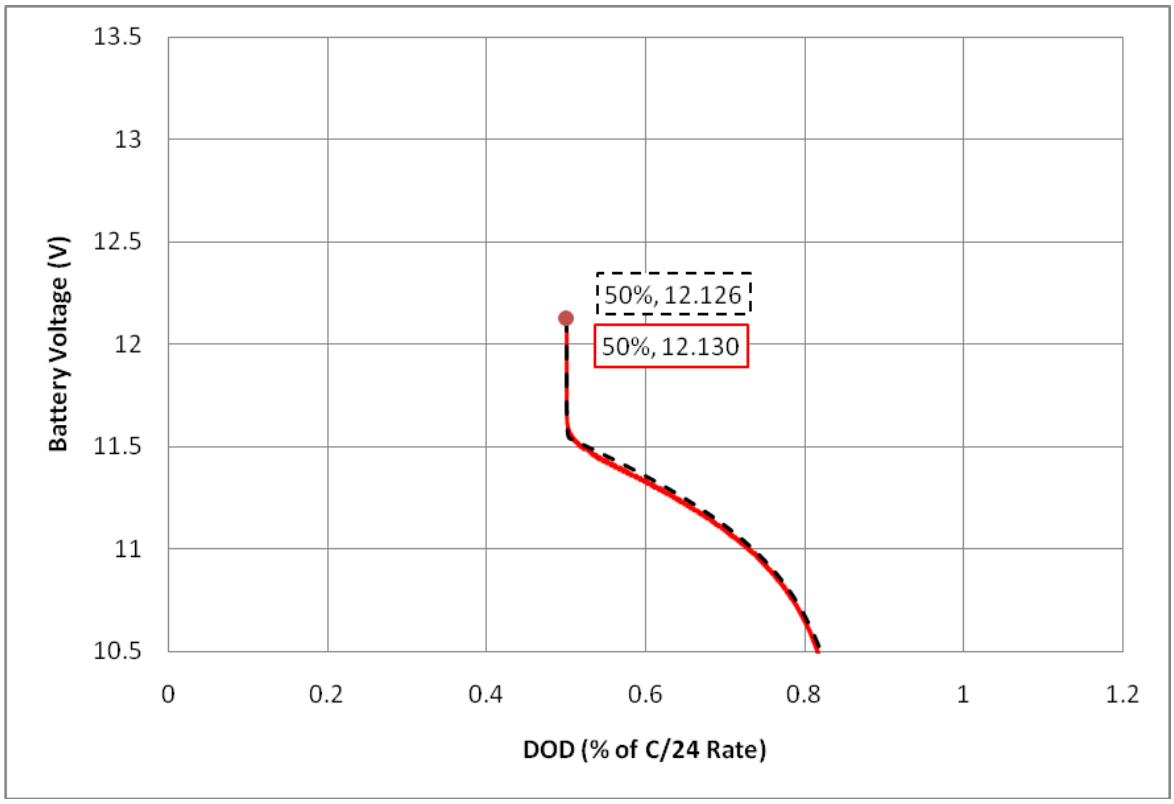

Fig 30 Discharge of the battery from 50% of SOC (Voltage versus DOD)

5.6 Task 6: Three-stage charging

The three-stage charging scheme is the most common way to charge a lead-acid battery. It includes bulk charging (constant current), absorbed charging (constant voltage) and float charging (small constant current to maintain the battery fully charged). The reason of switching to constant voltage is to keep the battery voltage below the gassing voltage, which will damage the battery and release dangerous hydrogen gas.

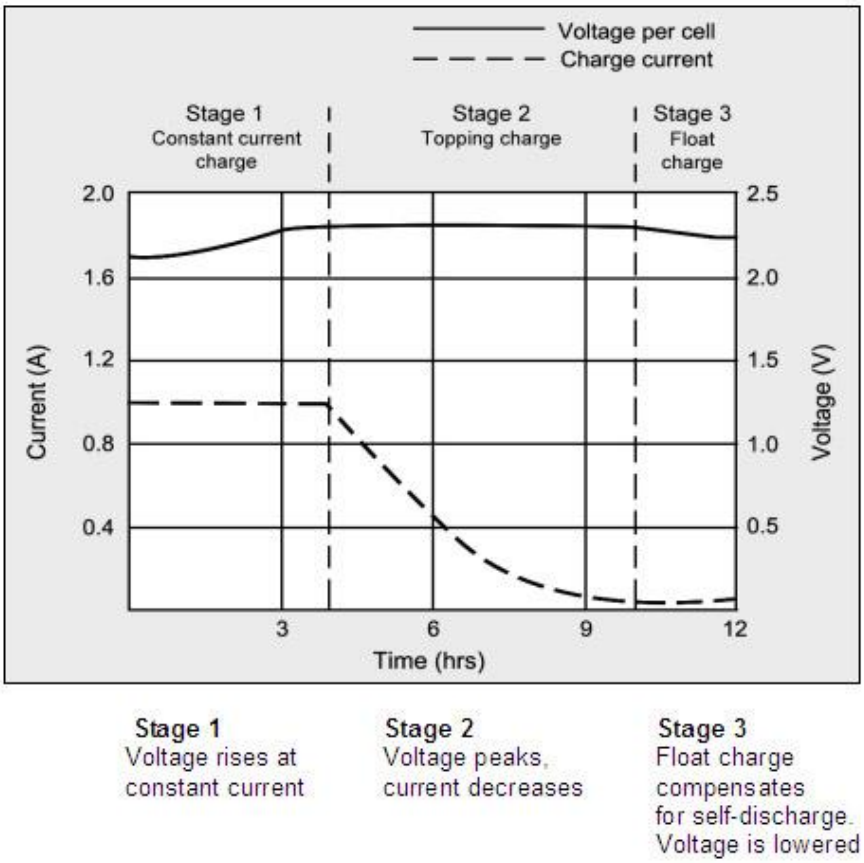

Fig 31 Charge stages of a lead acid battery [http://batteryuniversity.com]

From Fig.32 it can be seen that the voltage is constrained at a preset value of 14.2v when it gets high. The current drops until 0.8A which maintains the battery fully charged. The voltage curve during the constant current part has a similar shape with the discharging curves, except for a reversed y-axis and a different starting voltage. At constant voltage period, the current drops exponentially. For describing this continuous change current, a second order circuit model must be employed which is not discussed in the thesis.

This means the voltage curve for charging is very likely to be axially symmetric with the discharging curve. With this assumption, the model function can be derived from equation (10):

$$V_b(I,Soc) = Vs(t_0) + \frac{It}{C_s(I,Soc)} + IR_s^{'} + IR_t\left(1 - e^{-\frac{t}{R_tC_t}}\right) + V_c e^{-\frac{t}{R_tC_t}} \quad (12)$$

Equation (12) and equation (10) have similar components only with all the minus signs changed to plus signs. It is reasonable because if we set the direction of discharge current as positive, the charging process can be generally considered to be applying a negative current to a discharge function (the circuit model for both charging and discharging is the same).

In order to prove this assumption, a comparison between the plots of equation (12) and the experiment in Fig.32 is shown in Fig.33. For convenience, only the section with constant current is selected. The error for the test is 0.82%, the model curve nicely fits the real battery behavior.

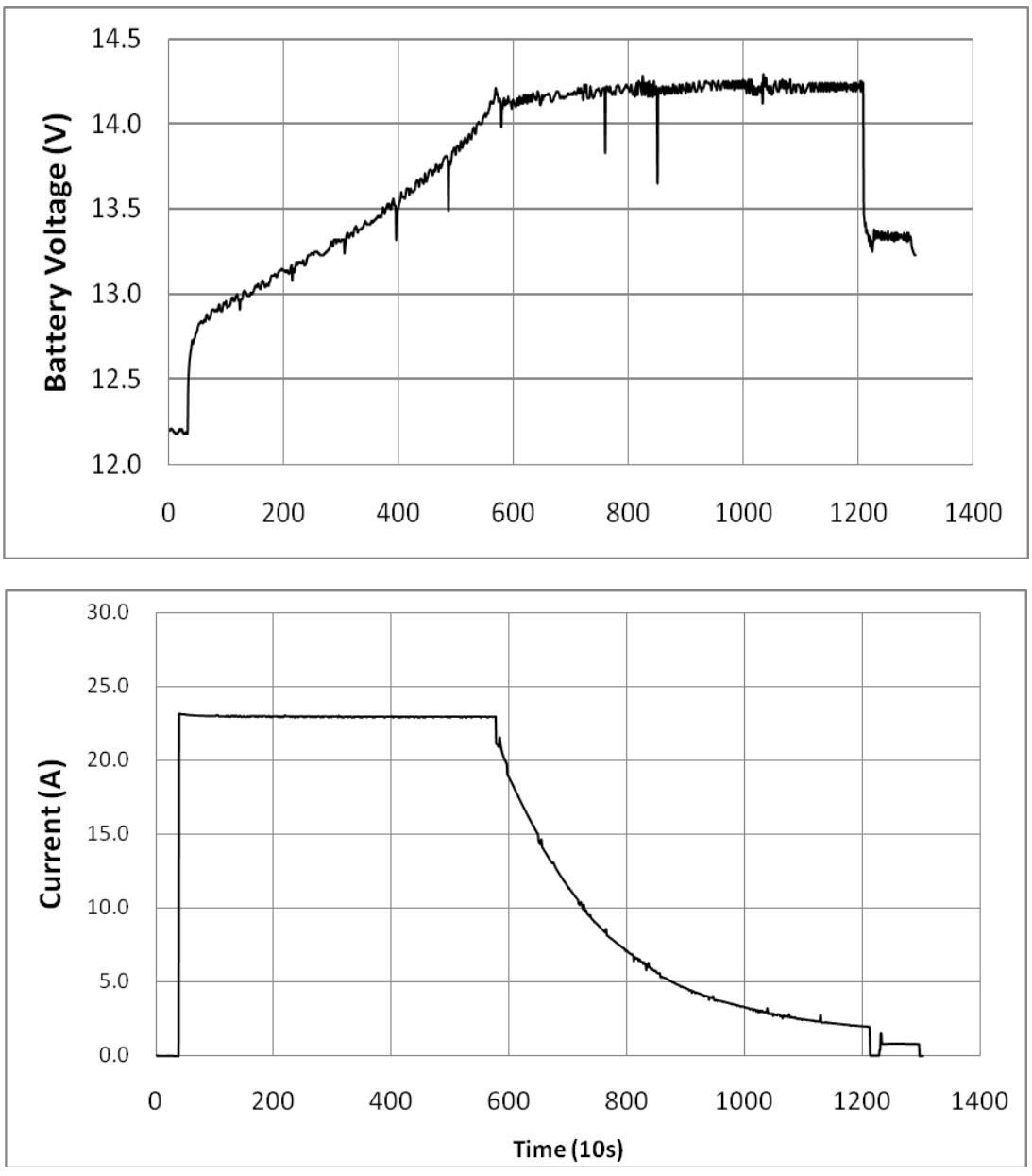

Fig 32 Result of three-stage charging by an auto charger

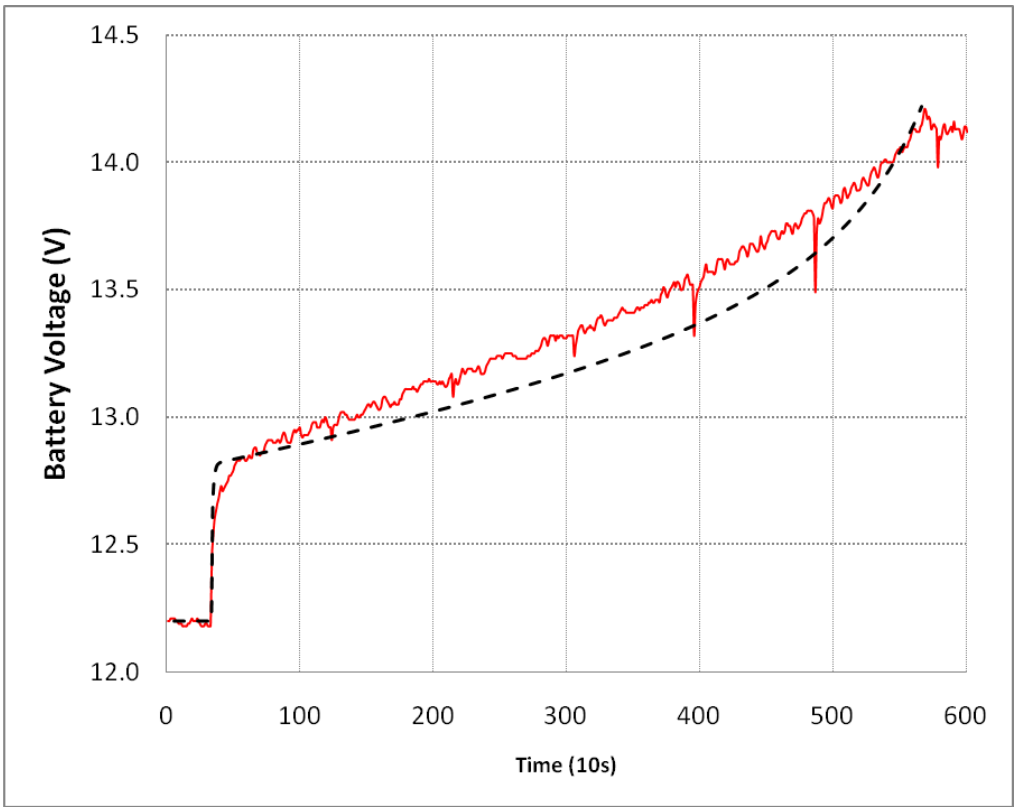

Fig 33 Comparison between test data and charging function

CHAPTER 6

TEMPERATURE EFFECT AND MODEL ANALYSIS

6.1 Temperature Effect on Self-discharge

Temperature influences chemical reactions dramatically. The rate change of these reactions affects the conductivity of the electrolyte and the movability of the charges. From a macroscopic view, it could be represented by the variation of the internal resistance and usalbe capacity. Theoretically, all the parameters for describing the battery are related to the temperature, the most significant affect is on the self discharge of the battery.

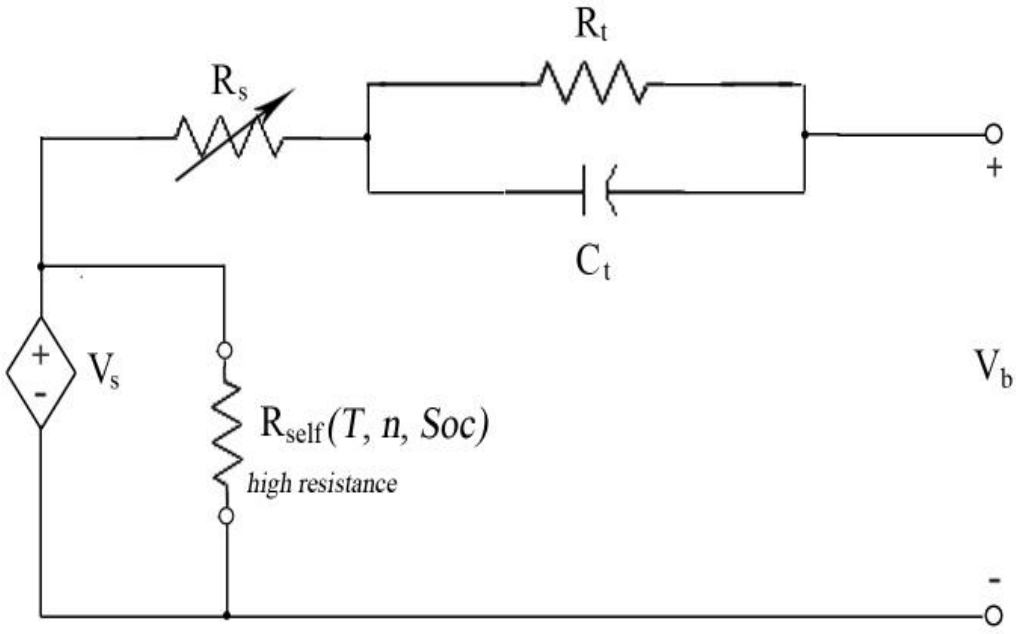

Fig 34 Circuit model with a parallel resistor R_{self}

A drop in capacity, or self-discharge, occurs during a cell's open circuit stand. This process takes place whether the electrodes are charged or discharged or standing without load. It is a phenomenon that the chemical reactions of the battery reduce the stored

charge without any connection between the electrodes. Self-discharge decreases the usable capacity of the batteries and causes them to have less charge than expected when actually put to use.

The effect of self-discharge can be embodied by an equivalent circuit using an element with high resistance in parallel with the main branch.

In Fig.34, a resistor R_{self} is added into the circuit model discussed in previous chapters. This resistor allows a very small current through which can be neglected when a normal discharge current is applied. But this parameter is highly related with the storage time of a battery.

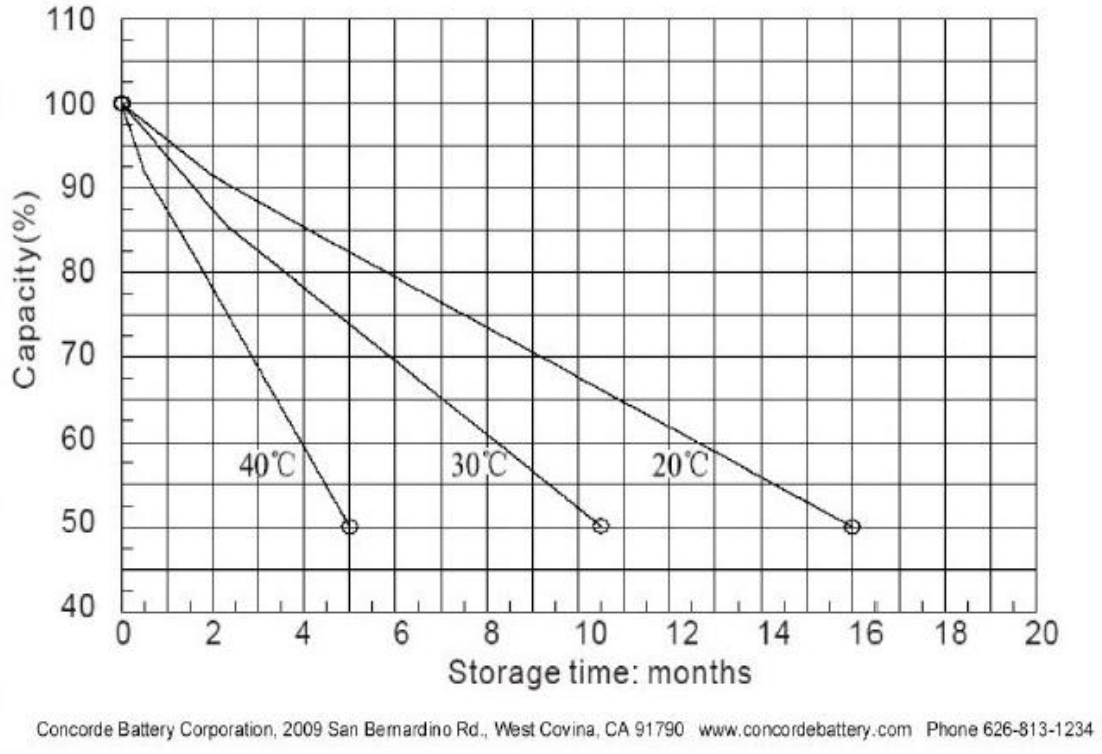

Fig 35 Self discharge characteristics [Concorde Technical Manual]

The self-discharge rate rises with an increasing temperature, from the data in Fig.35, the expression for R_{self} can be derived:

$$R_{self\cdot T} = 3.5291e^{-0.06T} R_{self} = V_b / i_{self\cdot T} \quad (13)$$

Equation (13) only gives the relation betweent R_{self} and temperature. Actually R_{self} is also affected by SOC and battery life cycles, but not as significant as the temperature.

6.2 Temperature effect on Battery Capacity

The usable capacity of the battery is also a function of temperature T according to the data in Fig.35. When the temperature drops below 25 ℃ the capacity drops from 100% to 20%. To reduce the complexity of the circuit model, we take the average values to make the capacity change linearly with temperature.

When T<25C, we have:

$$Dod_T = \left(1 - \frac{T-25}{65} \times 0.8\right) Dod = \left(1 - \frac{T-25}{65} \times 0.8\right)(1 - Soc) \quad (14)$$

if the temperature is higher than 25C and still in the normal range, its effect on capacity becomes so weak and can be ignored.

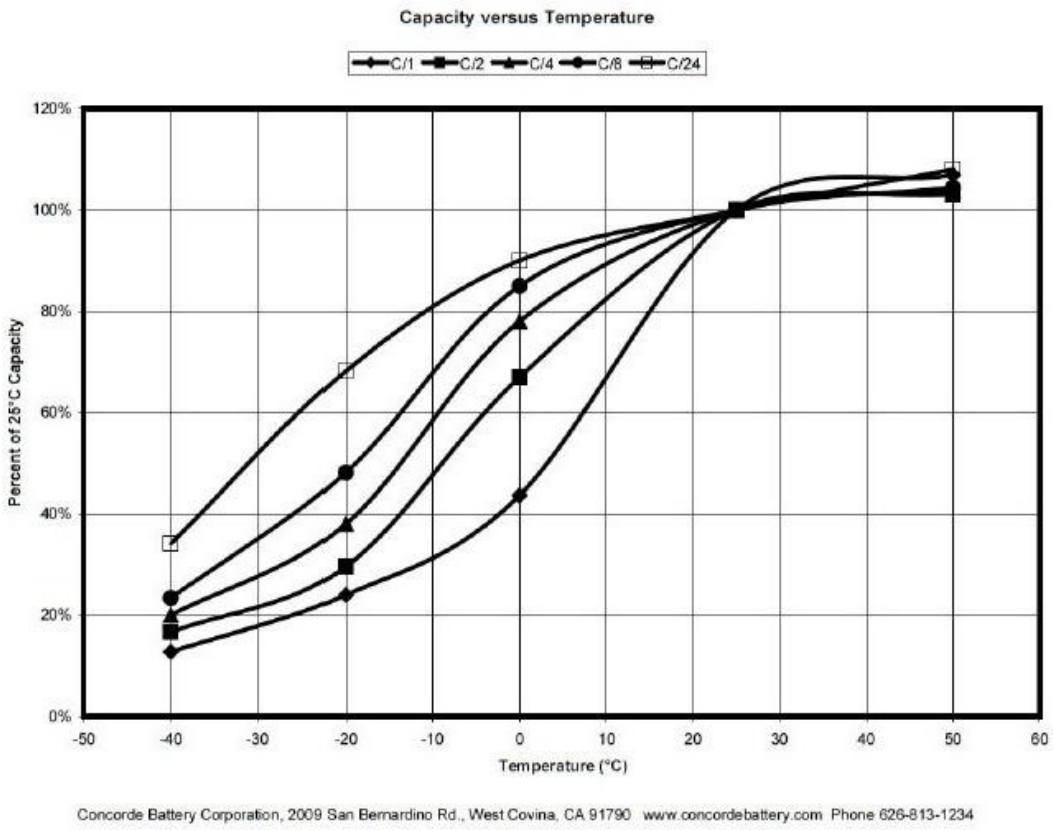

Fig 36 Temperature effects on battery capacity [Concorde Technical Manual]

6.3 Model Analysis

6.3.1 Finalized Model

Considering all the factors, the finalized form of the circuit model can be described by the following functions:

Discharging:

$$V_b(i,t) = Vs(t_0) - \frac{1}{C_S(i, Dod_T)} \int_{t_0}^{t} i(\tau)d\tau - [i(t) - i_{self}]R_s{}' - [i(t) - i_{self}]\left[R_t\left(1 - e^{-\frac{t}{C_t R_t}}\right)_2\right] - V_c e^{-\frac{t}{C_t R_t}} \quad (15)$$

Charging:

$$V_b(i,t) = Vs(t_0) + \frac{1}{C_S(i, Soc_T)} \int_{t_0}^{t} i(\tau)d\tau + [i(t) - i_{self}]R_s' + \left[i(t) - i_{self}\right]\left[R_t\left(1 - e^{-\frac{t}{C_t R_t}}\right)_2\right] + V_c e^{-\frac{t}{C_t R_t}} \quad (16)$$

Notice that in order to give a convenient look of the equation, the temperature effect on capacity or SOC of the battery is not directly shown. The DOD or SOC term is in the expression of Cs(I, DOD/SOC). I_{self} represents the current flowing through R_{self}, it's a small fraction of the current drawn from the source Vs. The independent variables of these two functions are current *i* and time t. Here *i* is not a constant, it could be any function of time. We didn't use the DOD or SOC as the independent variables because they themselves are also a function of time t.

6.3.2 Power Loss of Battery

With the derived model, a lot of features of the battery can be determined. The power loss during charging and discharge can be found by applying the total internal resistance.

$$P_{loss} = I^2R = I^2(R'_S + R_t)$$

The higher the SOC, the greater is the loss. And as the current increase, the power loss rises rapidly. If the battery is discharged at 4HR, which is 18.25A, the energy lost on the battery resistance is 0.092KWh. For the nominal 24HR discharging, the energy loss is 0.08KWh.

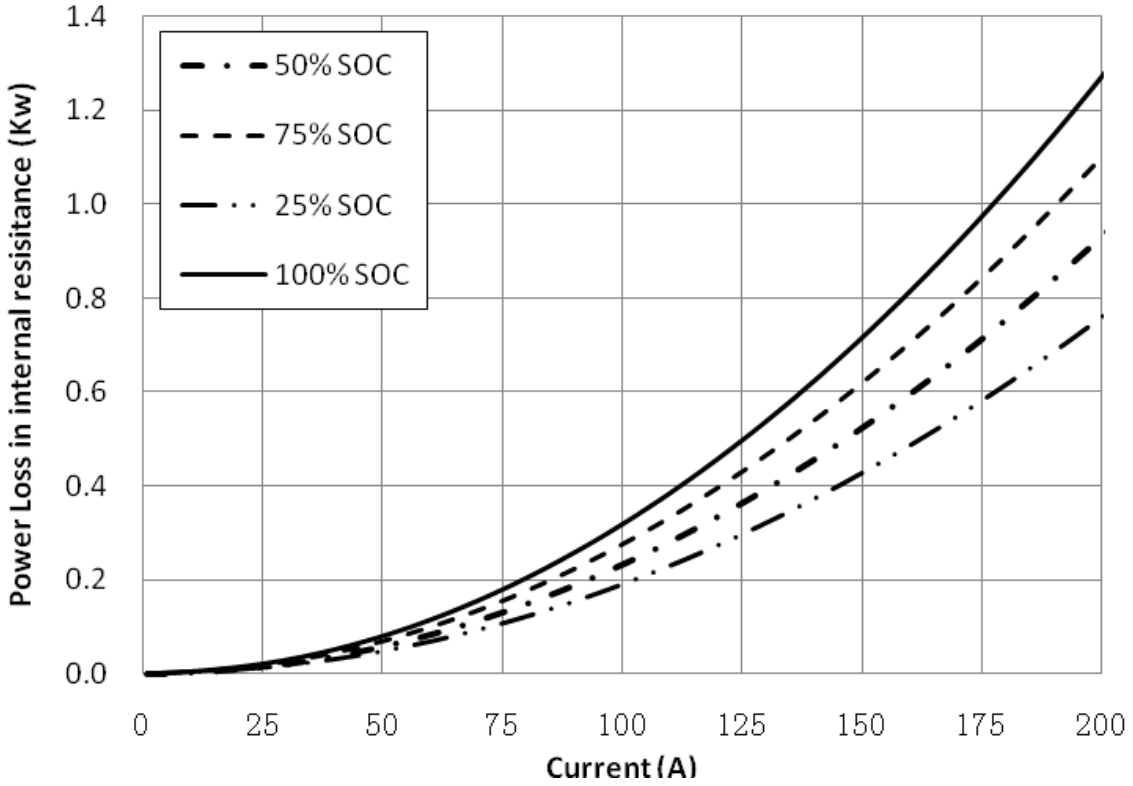

Fig 37 Power Loss during charging and discharging

These results will help further the research on battery efficiency. Knowing the relation between total discharge time and current rate will give a general idea of the average current applied in fast charging research, which is a hot topic nowadays. The fast charging algorithm requires large current pulses flow into the battery. In general, fast and uncontrolled charging leads to gassing and high temperature. Such dangerous situation can be avoided by a simulation test by employing this model to a designed computer program. So a general picture of the battery characteristics under high current will be demonstrated before going to the real experiment.

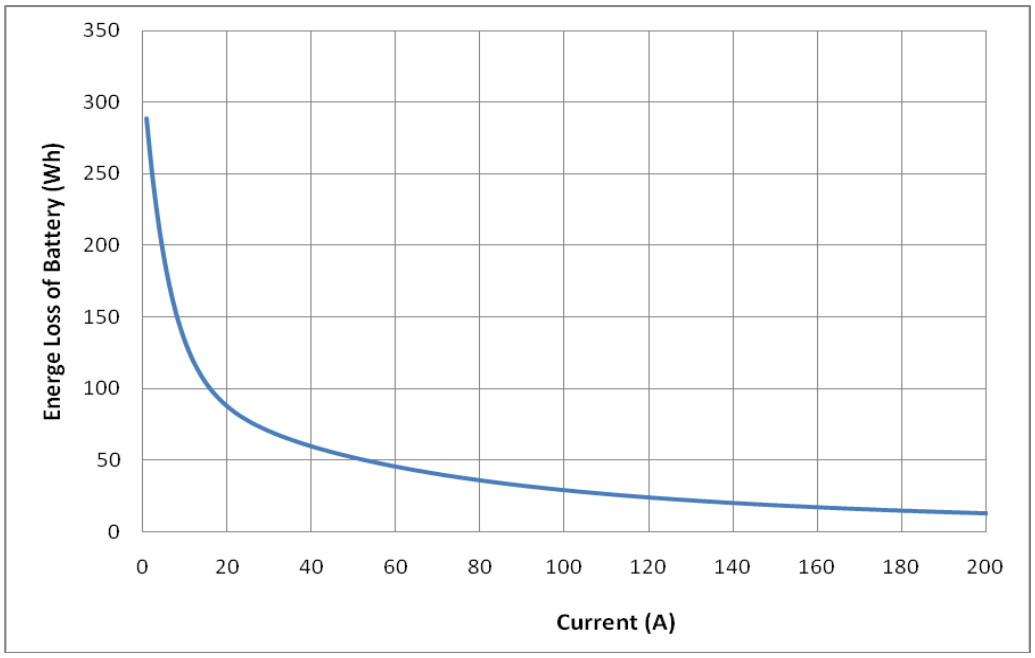

Fig 38 Total energy loss during a complete discharging process for each current rate

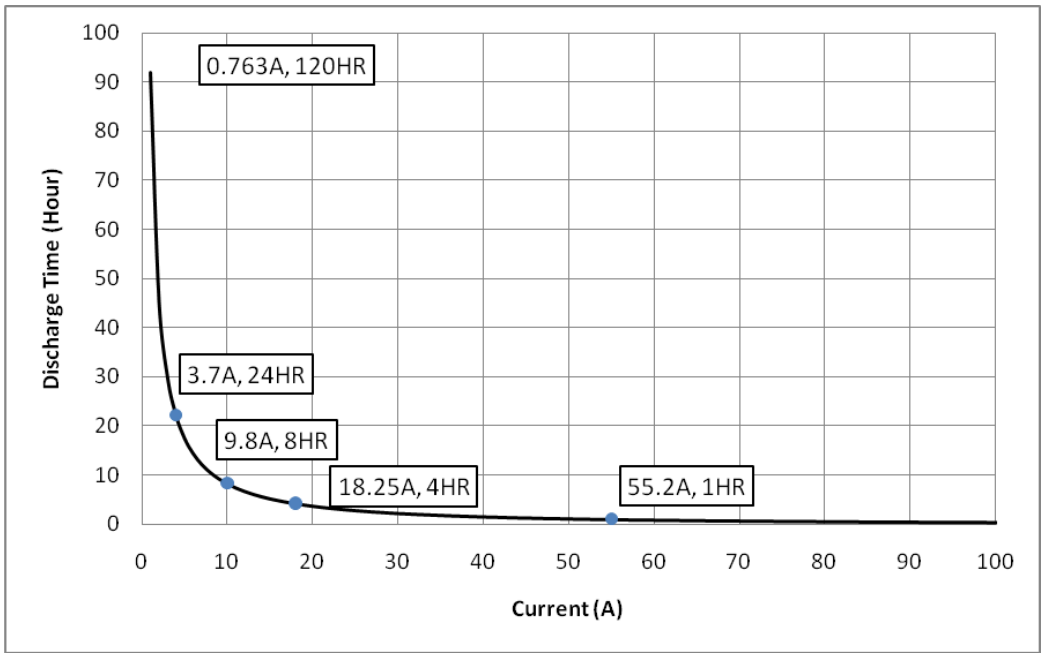

Fig 39 Relation between Discharge Time and Current Rate

6.3.3 Consideration of implementing more RC loops.

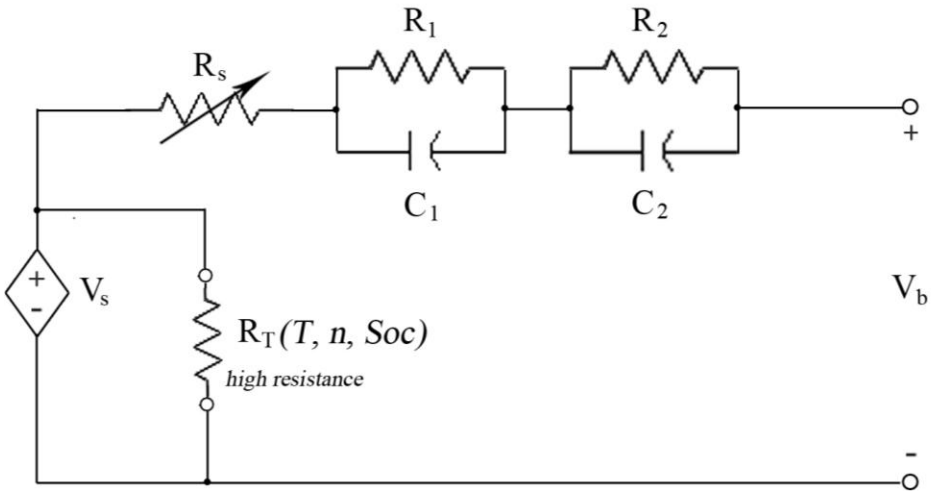

Fig 40 Circuit model with two RCs

The validation results in chapter 5 are not perfect, as has been discussed. The biggest problem is that every time when current goes from certain value to zero. It seems that the complexity of the circuit with a single RC loop can not be described well in the mode, especially at the end portion of each current pulse. The voltage always seems to need several hours to get stabilized. Therefore, more RCs are considered to be employed in the model.

Using more than one RC loop in the circuit model will increase the accuracy of the dynamic parameter derivation. In that case, the exponential zone of the battery will be split into two separate parts, and each of them with specific resistance and capacitance values, or time constants. In Fig 40, R_1C_1 and R_2C_2 are the two new time constant. The sum of R_1 and R_2 is equal to R_t, which means they are also a function of current and state of charge.

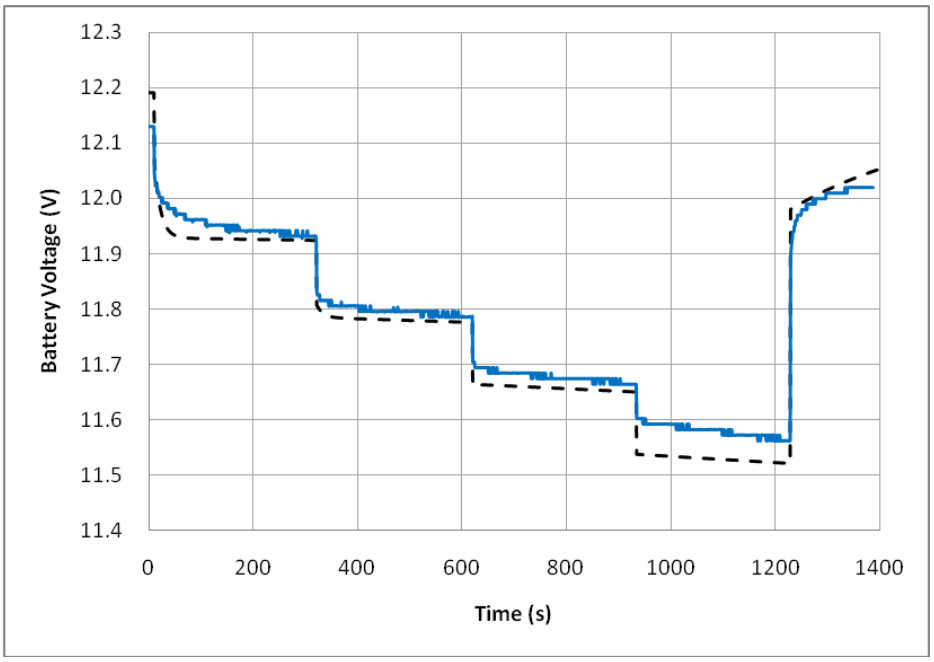

Fig 41 Simulation results using two RC loops for transient response.

Fig.41 shows the simulation results of using the two RCs model. In this simulation, R_1 is selected to be $0.8*R_t$ and R_2 is equal to $0.2*R_t$. The time constants are chosen to be 12 and 300 for R_1C_1 and R_2C_2 respectively. The voltage curve of the model fits the test result perfectly, at the very first current step (20A), but after that, the error range still increases. Above all, at the end part when the current switches from 5A to 0A, the model curve goes directly back to the starting voltage.

Therefore, although adding more transient components increase accuracy to a degree, it cannot solve the main problem of the model. Besides, adding more RCs increases the complexity of the model. To determine the parameters which represent accurately both current and battery SOC is difficult.

6.3.4 Simulation on MATLAB/SIMULINK

All the simulations in Chapter 5 of this thesis were carried out using both

MATLAB/Simulink and Excel 2007. Simulink is a good tool but unfortunately it doesn't include variable resistance in electrical components. The simulation results based on Simulink all use constant resistance. By manually changing the value of the resistor, we can achieve some important conclusions but it is not satisfactory. Besides, the resistance still has a linear relation with battery SOC. During charging or discharging, the SOC keeps changing with time and the resistance should also change with it, or the result will show greater error.

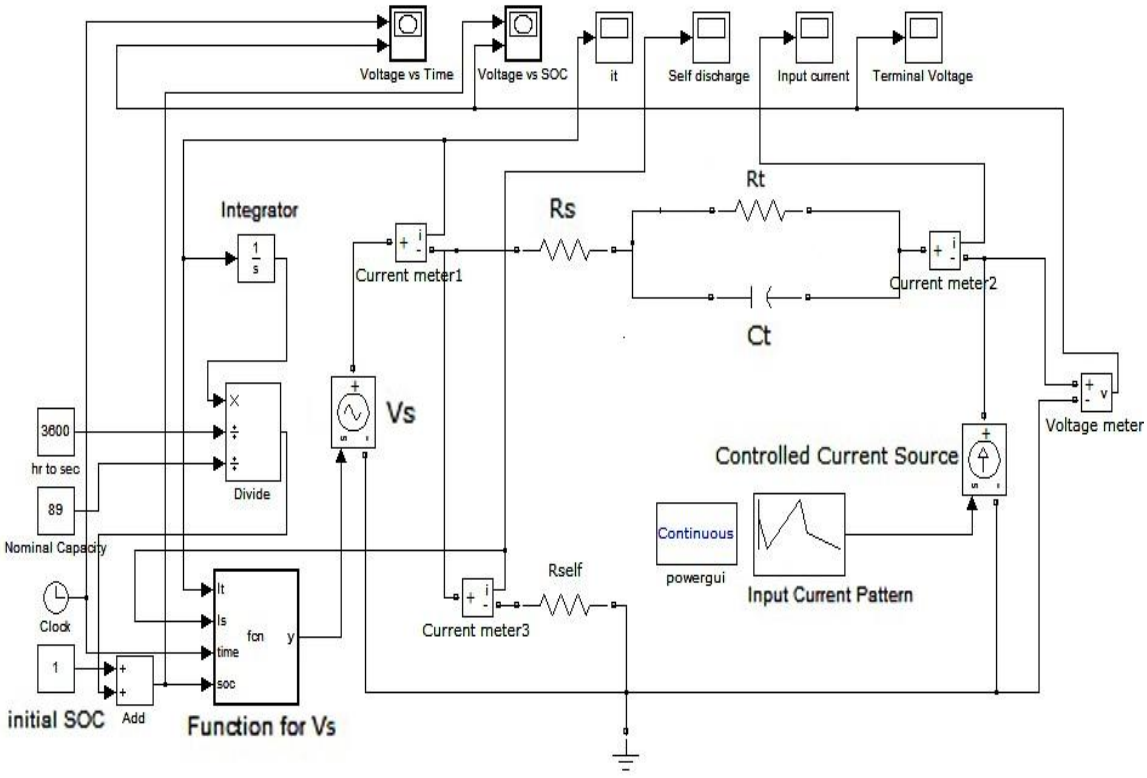

Fig 42 Suggested test model using MATLAB/Simulink based on final model

The Fig.42 gives a suggested test model using Simulink, the elements in the picture correspond to the ones in the circuit model. The controlled current source can supply any sequence of current. The Vs is set by the function block, which has multiple inputs. The

numbers in the left such as initial SOC and nominal capacity can be set to any value. The output displays on the top record all the important information of the circuit. If the resistors' values can be linked with a function block, the test model of this software would be perfect.

CHPTER 7

CONCLUSION AND FUTURE WORK

An accurate electrical model for AGM Lead-acid batteries has been developed. The battery function gives close agreement between experimental data and simulation results within an acceptable error range.

The temperature effect for the battery function is derived. It affects not only the storage time but also the available capacity of the battery. This result is based on the manufacturer's data because in the test the effect of temperature is not obvious enough to be observed.

Two RC loops are also considered but not taken into use in this model because of rise of complexity level. Increasing the number of electric elements in the model doesn't help match the curve when the current switches to zero. This may be affected by the property of the electrolyte and the separator material of the battery. Finding a universal function to describe this behavior is not obvious. Possibly a particular time constant could be used in the model function to improve the description. However, even if this will get a better result, the model is separated into two parts and not considered to be represented by a single function any more.

The simulation based on static parameter shows better results. The only source of the error is the polarization effect at the voltage drop when the battery stays in high SOC and using high discharge current. Considering implementing an inductor into the model is a

good idea, which will help demonstrate the voltage fluctuations at the beginning of discharging. This will significantly increase the complexity of this model since it becomes a second order circuit with several variables and it takes efforts to verify its mathematical solutions.

The complete model can be used to study on fast charging methods for lead acid batteries. High pulse current as an input will be applied. The characteristics during fast charging will be developed and studied to update the battery model. And this model can be a good reference for relevant research or applications.

REFERENCES

[1] Kong-Soon Ng, Chin-Sien Moo, Yi-Ping Chn, and Yao-Ching Hsieh, *"State-of-Charge Estimation for Lead-Acid Batteries Based on Dynamic Open-Circuit Voltage"*, 2nd IEEE International Conference on Power and Energy, 2008.

[2] Min Chen and Gabriel A. Rincon-Mora, *"Accurate Electrical Battery Model Capable of Predicting Runtime and I-V Performance*", IEEE Transactions on Energy Conversion, Vol.21, No.2, JUNE 2006.

[3] Ryan C. Kroeze, Philip T. Krein, *"Electrical Battery Model for Use in Dynamic Electric Vehicle Simulations*",Power Electronics Specialists Conference, 2008. PESC 2008. IEEE .

[4] Nosh K. Medora, Alexander Kusko, *"An Enhanced Dynamic Battery Model of Lead-Acid Batteries Using Manufacturer's Data"*, Telecommunications Energy Conference, 2006. INTELEC '06. 28th Annual International.

[5] Nosh K. Medora and Alexander Kusko, *"Dynamic Battery Modeling of Lead-Acid Batteries Using Manufacturers' Data"*, Telecommunications Conference, 2005. INTELEC '05. Twenty-Seventh International

[6] Michael Knauff, Jeffrey McLaughlin,Dr. Chris Dafis, etc. "*Simulink Model of a Lithium-Ion Battery for the Hybrid Power System Testbed*".

[7] Yoon-Ho Kim and Hoi-Doo Ha, *"Design of Interface Circuits with Electrical Battery Models"*, IEEE Transactions on Industrial Electronics, IEEE 1997

[8] Patrick J.van Bree, Andre Veltman, Will H. A. Hendrix, Paul P. J. van den Bosch, *"Prediction of Battery Behavior Subject to High-Rate Partial State of Charge"* IEEE Transactions on Vehicular Technology, Vol.58, No.2. Feb. 2009

[9] Olivier Tremblay, Louis-A. Dessaint, and Abdel-Illah Dekkiche, *"A Generic Battery Model for the Dynamic Simulation of Hybrid Electric Vehicles"*, Vehicle Power and Propulsion Conference, 2007. IEEE

[10] XueZhe.Wei, XiaoPeng.Zhao, YongJun.Yuan, *"Study of Equivalent Circuit Model for Lead-acid Batteries in Electric Vehicle"*, 2009 International Conference on Measuring Technology and Mechatronics Automation.

[11] Robert Rynkiewicz,*"Discharge and Charge Modeling of Lead Acid Batteries"* Linear Technology Corporation, Applied Power Electronics Conference and Exposition, 1999. APEC '99. Fourteenth Annual .

[12] C.-J. Zhan, X.G. Wu, S. Kromlidis, V.K. Ramachandaramurthy, M. Barnes, N. Barnes, N. Jenkins, *"Two Electrical Models of the Lead-acid Battery Used in a Dynamic Voltage Restorer"*, IEEE. 2003 proceedings online no. 20030124

[13] R.Prieto, J.A.Oliver, I.Reglero and J.A.Cobos, *"Generic Battery Model Based on a Parametric Implementation"*, Applied Power Electronics Conference and Exposition, 2009. APEC 2009. Twenty-Fourth Annual IEEE .

[14] Feng Xuyun and Sun Zechang, *"A Battery Model Including Hysteresis for State-of-Charge Estimation in Ni-MH"*, Vehicle Power and Propulsion Conference, 2008. VPPC '08. IEEE

[15] Zhou Su, Hu Zhe, Chen Feng-xiang, Zhang Chuan-sheng, *"Li-ion Battery System Modeling Based on Gassing Phenomenon"*, 1994-2010 China Academic Journal Electronic Publishing House.

[16] J.Marcos, J.Dios, A.M.Cao, J.Doval, C.M Penalver, A.Nogueiras, A. Lago, F. Poza Dpto. "*Fast Lead-Acid Battery Charge Strategy*", Applied Power Electronics Conference and Exposition, 2006. APEC '06. Twenty-First Annual IEEE

[17] Yi Ding, Robert Michelson, Woodstock, Charles Stancil, Marietta, *"Battery State of Charge Detector with Rapid Charging Capability and Method"*, United States Patent, No. 6,094,033

[18] http://www.sunxtender.com/pdfs/Sun_Xtender_Battery_Technical_Manual.pdf

VITA

Graduate College
University of Nevada, Las Vegas

Wenxin Peng

Local Address:
4248 Spencer St. apt 111
Las Vegas, NV 89119
USA

Degrees:
Bachelor of Science, Physics, 2009
Tongji University, China

Thesis Title:
Accurate Circuit Model for Predicting the Performance of Lead-Acid AGM Batteries

Thesis Examination Committee:
Chairperson, Dr. Yahia Baghzouz, Ph. D., P.E.
Committee Member, Dr. Rama Venkat, Ph. D.
Committee Member, Dr. Henry Selvaraj, Ph. D.
Graduate Faculty Representative, Dr. Robert Boehm, Ph. D., P.E.